MASTER

[redacted]

RECORD COPY

SNPO-C

Reilly

File 6.3

WANL-TME-768

July 1964

EE-3674

STRUCTURAL EVALUATION OF THE INNER REFLECTOR

(Title Unclassified)

DISTRIBUTION OF THIS DOCUMENT IS UNLIMITED

Astronuclear Laboratory

Westinghouse Electric Corporation

[redacted]

RECORD COPY

AUG 12 1964

DISCLAIMER

[redacted]
OF 1954

Westinghouse Electric Corporation

Astronuclear Laboratory Box 10864, Pittsburgh, Pa 15236
Telephone 892-5600

August 6, 1964

*Mr. R. W. Schroeder
Space Nuclear Propulsion Office
NASA Lewis Research Center
21000 Brookpark Road
Cleveland 35, Ohio

Subject: WANL-TME-768, "Structural Evaluation of the Inner Reflector," dated July 1964

Dear Mr. Schroeder:

Transmitted herewith are three (3) copies of the subject report. This report is transmitted for your information.

Respectfully,

H F Faught

H. F. Faught
Program Manager
NERVA Nuclear Subsystem

Enclosures - 3

cc: Mr. R. Wilke, SNPO-C Resident Office at WANL
Mr. G. O'Brien, SNPO-C Resident Office at WANL

WHEN SEPARATED FROM ENCLOSURES, HANDLE THIS DOCUMENT AS UNCLASSIFIED
(INSERT PROPER CLASSIFICATION)

[redacted]
OF 1954

[redacted]
Atomic Energy [redacted]

COPY NO. 6

SNPO-C

Astronuclear

WANL-TME-768

July 1964

EE-3674

79

MASTER

Submitted by:
Westinghouse Electric Corporation
Astronuclear Laboratory
P. O. Box 10864
Pittsburgh 36, Pennsylvania

~~Group 1~~
~~Excluded From Automatic Downgrading and Declassification~~

Prepared by:

W. G. Parker
W. G. Parker
Engineering Mechanics

~~INFORMATION CATEGORY~~

~~Confidential Restricted Data~~
~~W. J. Rowan 7/17/64~~
~~Authorized Classifier (Date)~~

Classification cancelled (~~or changed to~~)
by authority of
by H. A. C TIC, date SEP 11 1973

Approved:

E A Watjen 7/17/64
E. A. Watjen, Supervisor (Date)
Core Components and
Thermal Experiments

W. J. Rowan 7/17/64
W. J. Rowan, Manager (Date)
Engineering Mechanics
Experimental Engineering

STRUCTURAL EVALUATION
OF THE INNER REFLECTOR

(Title Unclassified)

Reviewers	Class.	Date
DBW	U	5-6-82

SPECIAL RE-REVIEW
FINAL
DETERMINATION
Class: U

/als

[redacted]

AUG 12 1964

TABLE OF CONTENTS

LIST OF FIGURES

Figure

LIST OF TABLES

1.0 SUMMARY

1.1 During operation of the nuclear reactor engine, the inner reflector graphite cylinder is subjected to an axially varying pressure distribution. Compressive stresses of sufficient magnitude to cause instability and failure are possible. A series of experimental investigations were therefore required to substantiate the structural integrity of the inner reflector.

1.2 Test data is presented describing the structural design integrity of the inner reflector graphite cylinder (Part No. 936J568K04P). Tests were designed to subject the reflector to uniform pressure differentials along its outer periphery to determine the rate of gas diffusion (permeability rate) through the wall thickness for pressure ranges of 0 to 100 psig and the structural integrity of the reflector at pressure ranges from 0 to 200 psig. The reflector was also subjected to a series of simulated pressure load environments of the reactors. All tests were conducted at ambient temperature.

1.3 Results from these tests indicate that the design of the inner reflector is satisfactory for NRX-A1 and NRX-A2 reactor operation. Permeability tests indicated that the inner reflector should be impregnated following the final machining operation. Uniform pressurization tests to 200 psig give evidence that the inner reflector will likewise perform satisfactorily during NRX-A3 reactor operation. However, a test to directly simulate the NRX-A3 pressure load environment (not possible with the present test rig) will be conducted at a future date.

2.0 INTRODUCTION

2.1 A primary component of the NRX-A nuclear reactor is the inner reflector graphite cylinder. (The inner reflector is a hollow right circular cylinder approximately 54 in. in length with an inner diameter of 36 in. and an outer diameter of 39.8 in. Various grooves, slots, and holes are machined into the cylinder as shown in Figure 1.) The inner reflector functions primarily as a neutron reflector between the graphite core and the outer beryllium reflector. In addition to this reflector function, it serves as a flow barrier between core flow and reflector cooling flow, a thermal and pressure barrier between the core and the outer reflector, an absorber and transmitter for the core lateral loads and a retainer for the filler strips. (Reference 1)

2.2 The many functions and environments of the inner reflector cylinder, as well as its intricate machined shape, severely hampers accurate detailed design analysis. A series of experimental investigations were therefore required to substantiate the structural integirty of the reflector.

2.3 During reactor operation, the inner reflector is subjected to an environment of hydrogen gas. Excessive diffusion of this gas through the reflector wall, could result in a compromise of structural reactor integrity. A series of permeability tests were therefore performed at ambient temperatures on samples of reflector material and on the inner reflector in environments of nitrogen and hydrogen gases.

2.4 As a result of the gaseous environment imposed upon the reflector during reactor operation, a pressure drop exists along the length of the outer periphery. It is possible for this pressure drop to vary from 0 psi at the dome end to approximately 190 psi at the nozzle end of the reactor. Large compressive stresses could result at the inner periphery of the reflector of sufficient magnitude to cause instability and possible failure. A series of buckling tests were therefore performed on the reflector to determine its structural integrity. These tests consisted of ramp pressurization of the inner reflector and encompassing simulated core support barrel (the core support barrel is an aluminum shell that shrinks onto the reflector during cold gas flow due to its high coefficient of thermal contraction) simulating the anticipated pressure drop in the NRX-A1 and NRX-A3 reactors. (The pressure drop in the NRX-A2 reactor is similar to that obtained during NRX-A1 reactor operation.) (Figure 2) The inner reflector was also subjected to a uniform external pressure of 200 psig (no simulated core support barrel used), a condition which is felt to be more structurally severe than the ramp pressure distribution.

2.5 A porous flow test of the inner reflector cooling holes was performed to accumulate data for aiding in the evaluation of the NRX-A1 pressure probe and the plugged core (G-3) pressure probe test results. (The axial cooling holes of the reflector are used as a part of the channels for pressure probes into the seal chambers of the NRX-A1 and plugged core (G-3) tests.)

2.6 The objectives of these tests were to determine the pressure and flow rate in a cooling hole of the reflector during uniform external pressurization of the reflector and the gas permeability rate of the reflector during internal pressurization of a cooling hole.

2.7 During the permeability and buckling tests described above, the inner reflector strains (at the inner periphery), deflection modes, and permeability rates were recorded at each pressure test level.

3.0 CONCLUSIONS AND RECOMMENDATIONS

3.1 The following conclusions can be drawn from tests performed on the inner reflector graphite cylinder:

3.1.1 The design of the inner reflector is satisfactory for withstanding the anticipated pressure load environments of the NRX-A2 reactor. All testing was performed at ambient temperatures.

3.1.2 Initial testing of the inner reflector indicated a high gas diffusion rate through the wall at low pressures. Reimpregnation of the inner reflector resulted in a large decrease (a factor of 80 at 10 psig) of the gas diffusion rate. It is therefore concluded that impregnation of the inner reflector should be performed following the final machining operation.

3.1.3 The present test pressure vessel used for inducing pressure levels to the inner reflector was not entirely satisfactory for simulating NRX-A3 test conditions.

3.1.4 Although some permanent deformation (approximately 40 mils on the radius) of the reflector occurred during uniform pressurization to 200 psig, the result would not significantly influence reactor operation. Since this loading condition is felt to be more structurally severe than a ramp pressurization test, it gives evidence that the inner reflector will perform satisfactorily during NRX-A3 reactor tests.

3.2 The following recommendations are presented for future testing:

3.2.1 A pressure vessel be designed to allow subjecting the inner reflector to simulated NRX-A3 and NRX-A5 test conditions.

3.2.2 To aid in designing future reactors, a test should be performed wherein the inner reflector, under simulated reactor conditions, is tested to failure for ramp and uniform pressure loads.

4.0 TEST DESCRIPTION

4.1 The inner reflector graphite cylinder was subjected to a series of permeability and buckling tests.

4.2 The purpose of the reflector permeability tests was to determine the gross rate of nitrogen and hydrogen diffusion through the wall of the inner reflector (Appendix B). The reflector was placed in a steel pressure vessel (Figure 21). The chamber between the vessel and the cylinder was pressurized using nitrogen and hydrogen gases. (The flow of gas necessary to maintain the test pressure differential across the barrel thickness represents the permeability rate.) The barrel permeability rate, strains, and deflections were monitored at each test pressure level. Also, in conjunction with these permeability tests, a related permeability test was performed on the inner reflector cooling holes to accumulate data for aiding in the evaluation of NRX-A1 and G-3 pressure probe test results (Appendix C). This test consisted of externally pressurizing the reflector using nitrogen and hydrogen gases (0 to 100 psig) and measuring the pressure and gas flow rate in a peripheral cooling hole. The cooling hole was then internally pressurized (0 to 100 psig; no external pressure) and the permeability rate of the barrel determined.

4.3 The purpose of the buckling tests was to determine the structural integrity of the inner reflector when subjected to a ramp and uniform pressure distribution. A nitrogen gas environment was used to produce the desired pressure profiles. The ramp pressurization test of the reflector (Appendix D) was performed by thermal shrinking the simulated core support barrel onto the inner reflector and then pressurizing the outer surface of the support barrel in steps with nitrogen gas (Figure 2). Thus, the reflector was subjected to a uniform pressure (shrink fit pressure) plus a ramp pressure. The uniform pressure buckling test of the inner reflector was performed in the same manner as the permeability tests using a nitrogen gas environment. However, the pressure range for this test was 0 to 200 psig.

5.0 DATA ANALYSIS

5.1 The inner reflector graphite cylinder was subjected to a series of permeability and buckling tests. These tests were designed to substantiate the operational integrity of this component during the NRX-A1 and NRX-A2 reactor test series. An attempt was also made to subject the reflector to operating conditions anticipated during NRX-A3 reactor tests.

5.2 Permeability Tests

5.2.1 The first tests performed on the reactor were a series of permeability studies using hydrogen and nitrogen gas environments. The results from these tests indicated flow rates of 2.32 lb/min for 10 psig nitrogen gas pressure and 1.04 lb/min for 22 psig hydrogen gas pressure. These flow rates were extremely high when compared with tests performed on samples of impregnated barrel material (Reference 2). During the manufacturing process the reflector is impregnated with a silica-based solution (35% SiO_2 in H_2O) to minimize its porosity; then machined to its final configuration. The high flow rates obtained from these tests indicated that part of the impregnating material was removed during the final machining process giving rise to porous areas in the reflector. The inner reflector was returned to the manufacturer to undergo a re-impregnation process so that future tests performed on the reflector would yield meaningful results.

5.2.2 After completion of the re-impregnation process, the reflector was returned to the laboratory for further testing. Two permeability tests using nitrogen gas and one low pressure test using hydrogen gas were again performed on the graphite barrel. The first nitrogen gas test was terminated at 30 psig due to a defect in the material used for sealing the dome end of the reflector. After repairing the seal, a second nitrogen test run was made which had to be terminated at 40 psig due to excessive leakage past the plugs used to prevent gas flow through the plunger holes. While inspecting these plugs, a longitudinal crack was discovered in the third lateral support seal segment groove from the dome end of the reflector. The crack was limited to the area of the groove running from one stress relief radius to the opposite stress relief radius but not extending into the heavy land on each side of the groove. (Figure 3) A stress of about 600 to 700 psi in the cracked area was recorded which was not of a sufficient magnitude to cause the failure. A low pressure check with nitrogen gas using leak-tec as indicating agent showed some increase in gas leakage through the cracked area but not of a sufficient magnitude to indicate that the crack would extend completely through the barrel. Following a low pressure hydrogen gas permeability test the barrel was visually examined for an increase in the extent of the crack. No change was apparent.

5.2.3 Even though excessive leakage occurred, in the area of the plunger holes during these tests, the gross permeability rate for the reflector, after the re-impregnation process, was approximately an order of magnitude less than previous values obtained (0.25 lb/min at 10 psig nitrogen gas pressure and 0.15 lb/min for 22 psig hydrogen gas pressure). A new plunger hole gas sealing arrangement was designed before proceeding with further tests.

5.2.4 The graphite barrel was removed from the test vessel and the external surface of the reflector inspected thoroughly in the area of the internal crack. No evidence of cracking was visible on this surface. A probe inserted into the longitudinal cooling holes revealed an obstruction in the hole in the cracked area. Since it was known that during the reaming operation of these holes following re-impregnation a drill bit had broken off in one of the holes, it was conjectured that this obstruction was the broken bit. X-rays taken of the area proved this to be correct and also showed considerable additional delamination cracks in the same area. (See attached sketch made from x-ray plate, Figure 4.) This led to the conclusion that the crack occurred as a result of the breaking of the drill bit and was not directly attributable to the stresses induced by the pressure loading. During the remainder of the test series considerable attention was given to reflector cracking, the results of which will be discussed later.

5.2.5 Having obtained a sufficient gas sealing plug for the plunger holes, the inner reflector was again tested for permeability using nitrogen and hydrogen gases. Two nitrogen gas tests were performed on the barrel. For the first test (0-100 psig pressure), the permeability rate was below the measurable capacity of the instrumentation. For the second test, permeability data was obtained for gas pressures of 0 to 140 psig (Table I). Results indicate a flow rate of 0.594 lb/min at 140 psig. For the hydrogen gas test, reflector permeability data was obtained for pressures of 0 to 100 psig (Table I). Results from this test indicated a flow rate of 0.092 lb/min at 100 psig.

5.2.6 A graphical representation of the data obtained from the hydrogen and nitrogen gas reflector permeability tests is given in Figure 5. Comparing this data with that obtained prior to re-impregnation (2.32 lb/min at 10 psig nitrogen gas pressure and 1.04 lb/min for 22 psig hydrogen gas pressure) indicates a reduction of the flow rate resulting from the re-impregnation process by a factor of 80 for the nitrogen gas (at 10 psig) and 70 for the hydrogen gas tests (at 22 psig).

5.2.7 From the above series of permeability tests it can be concluded that the inner reflector gas flow rates can be greatly minimized by impregnating the barrel following the final machining operation.

5.3 Buckling Tests

5.3.1 A series of pressure buckling tests were conducted on the inner reflector as a prerequisite requirement of the NRX-A1 test program. The purpose of these tests were to substantiate the structural integrity of the inner reflector cylinder when subjected to pressure differentials anticipated during the NRX-A1 and NRX-A2 test series. An attempt was made to subject the inner reflector to pressure differentials anticipated during the NRX-A3 tests. A test was also performed where the inner reflector was subjected to a uniform external pressure of 200 psig, a condition which is felt to be more structurally severe than the NRX-A1, NRX-A2, or NRX-A3 pressure profiles.

5.3.2 Prior to performing the tests simulating the NRX-A1 pressure profile, (ambient and split-flow conditions, Figure 2), an aluminum sleeve (0.063 in. thick) simulating the reactor core support barrel was shrink-fitted on the inner reflector. Ramp pressure simulation of NRX-A1 conditions was then applied to the surface of the aluminum barrel. Typical strain gage and LVDT deflection data plots are shown on Figures 6, 7, 8 and 9. These data were recorded in the maximum pressure chamber at the nozzle end of the barrel and are the highest expected.

5.3.3 Investigation of all other strain and deflection data along the length of the barrel showed no unusual readings. These values were all lower than the above because of the smaller pressure differential. Since the split-flow pressure requirements were applied as an addition to the ambient flow pressures, the first four test chambers for applying ramp pressures from the dome end of the reflector were identical for both tests. Therefore, representative maximum data points for any pressure can be picked off of the curves presented in Figures 6, 7, 8 and 9. The peripheral compressive strain readings taken next to the plunger hole (Figure 9) drilled in a groove were slightly higher due to stress concentrations as compared to the readings in the parent groove material (Figure 7). The deflection data was very uniform and did not indicate any measurable instability (Figure 8).

5.3.4 The shrinking of the aluminum sleeve onto the outer diameter of the graphite barrel induces additional stresses to the ones recorded during testing. These stresses are calculated as described in Appendix A to be 686 and 871 $lb/in.^2$ in the land and groove areas respectively. By converting the recorded test strains to stress using an $E = 1.5 \times 10^6$ psi and adding the calculated shrink stress values to these, the approximate maximum stresses experienced by the reflector were 2650 $lb/in.^2$ in the land and 2700 $lb/in.^2$ in the groove respectively. The combined effects of the Poisson's stress and some secondary stress due to the complex geometry near the plunger holes are recorded on gage 9 and 10 (Figure 9).

5.3.5 It was concluded from this series of tests that the inner reflector graphite cylinder will meet the static structural requirements of the NRX-A1 or NRX-A2 test environments.

5.3.6 An attempt was made to simulate the anticipated pressure profile imposed on the inner reflector during the NRX-A3 test series. However, at 150 psig the rubber seal separating the seal chamber at the nozzle end of the reflector and an adjacent one failed to function thereby causing a decrease in pressure in the nozzle chamber. The test was aborted at this point since simulation of NRX-A3 conditions were no longer possible. Strain readings obtained at the nozzle end of the reflector were approximately 1300 μ in./in/ in the land. Values obtained during NRX-A1 operating pressure simulation. Since the present test vessel was not capable of simulating NRX-A3 conditions, a new test vessel having the capacity of ramp pressurization to 600 psig and uniform pressurization to 1000 psig of the reflector is currently being designed.

5.3.7 Two uniform external pressurization tests were performed on the inner reflector using nitrogen gas to evaluate its structural integrity. The first test was terminated at 150 psig due to high compressive strains (3400 μin./in.) adjacent to the cracked area of the reflector. Also, elliptical deformation of the reflector became apparent at 130 psig when when the deflection pattern (radially inward) of the reflector reversed. It was felt that the combined effect of the above could result in possible failure of the reflector at higher pressure levels; however, in order to completely substantiate the operational integrity of the reflector, a test to 200 psig uniform pressure was mandatory.

5.3.8 A tabulation of the data obtained from pressurizing the reflector to 200 psig is given in Tables II and III. (Strain gage data are average values obtained from all uniform pressure tests performed on the reflector except where noted.) Graphical representations of selective pieces of data are shown in Figures 10, 11, 12 and 13.

5.3.9 The maximum strain occurring in the reflector at 200 psig was 4121 μ in./in. in the second land from the nozzle end. Converting this value to stress, using Figure 14, the maximum stress in the reflector was 3700 psi. It can be shown by simple thick wall cylinder analysis that the theoretical maximum stress, neglecting stress concentrations, will occur at the inner periphery of the land. Stress concentrations around the plunger holes (Table III) are experimentally shown to magnify the gross material stress in the areas considered by approximately 1.08 at the second groove from the nozzle end and 1.20 at the tenth groove. The difference between these two magnification factors probably results from the 16,900 lb axial load at the ends of the reflector and its deflection modes. Also, from Table III, a difference at approximately 3 exists between the strain values determined at the sides of the plunger holes and the bottom of the holes. This difference can be explained - the following reasoning suggests an approximate methods of analyzing the stress distribution in the plunger hole area - by considering the case of a simple plate with a center circular hole in compression (Reference 2). Comparing the theoretical stress at the bottom of the hole with the stress in the direction of loading a short distance from the hole, we find a factor of 3 existing. The placement of the strain gages in this test corresponds with the theoretical stress placement definitions and therefore gives some reasoning behind the factor of 3 occurring in the experimental strain results.

5.3.10 The deflection data obtained from this test (Figure 13) again indicated unsymmetrical deformation of the reflector. At 130 psig a reversal in the direction of deflection readings occurred which continued to increase in magnitude throughout the test. It is felt that the unsymmetrical deformation of the reflector resulted from the reflector being initially non-circular and the fact that the material constants vary from point to point throughout the reflector.

5.3.11 Upon reaching 200 psig pressure, a malfunction in the test equipment resulted in the external pressure applied to the reflector dropping to 0 psig. Radial deflection readings taken then, and compared with initial values, were found to differ by 26 to 38 mils. Since a complete dimensional history of the reflector was available prior to this test, another series of dimensional measurements were obtained and compared with previous data in order to determine if permanent deformation of the reflector had resulted through testing to 200 psig. Results of this investigation are tabulated in Appendix E. The results indicate radial differences of approximately 10 to 40 mils depending upon circumferential position. These results therefore show that some permanent deformation of the reflector occurred during pressurization to 200 psig.

5.3.12 As was stated earlier, x-ray examination of the reactor was performed after detecting cracking in the third lateral support seal segment groove from the dome end. Prior to performing the above series of buckling tests, x-rays were again taken of the cracked area (Figure 15) to determine if the ramp pressurization tests had resulted in further cracking. Results from these x-rays indicated that the original cracks had lengthened approximately one half in. ($\frac{1}{2}$) and that new cracks had occurred in the area adjacent to the broken drill bit. After uniformly pressurizing the reflector to 200 psig, another series of x-rays were taken for comparison with the above. These x-rays indicated that no apparent additional cracking occurred during uniform pressurization to 200 psig. Since the reflector was under a state of approximate uniform compression during this test, these results are reasonable. It should be pointed out that during the ramp pressurization of the reflector, an axial bending moment is superimposed upon the compression loading. This axial moment probably resulted in the additional delamanation and cracking that occurred during the ramp pressure cycle.

5.3.13 Although some permanent deformation occurred during the above series of buckling tests, the extent of the deformation was small. Cracks that had previously been observed in the reflector did not significantly affect the test results. It can therefore be concluded that the inner reflector can satisfactorily function as designed during reactor operation.

5.4 Cooling Hole Porous Flow Tests

5.4.1 In conjunction with the permeability tests on the inner reflector, a test was performed on the cooling holes of the reflector to accumulate data for aiding in the evaluation of the NRX-A1 and G-3 pressure probe test data. The purposes of these tests were to determine the pressure and flow rate in a cooling hole during external pressurization of the reflector and the permeability rate of the reflector during internal pressurization of a cooling hole. Data obtained from these tests are summarized in Tables IV and V. Figures 16 through 20 summarize the data graphically.

5.4.2 At 100 psig external pressure, the gross permeability of the barrel was 0.427 lb/min for nitrogen gas and 0.0995 lb/min for hydrogen gas. These values compare to 0.376 lb/min for nitrogen gas and 0.092 lb/min for hydrogen gas at 100 psig obtained during previous permeability testing of the inner reflector. The discrepancies in these data can probably be attributed to test rig assembly and the small amount of permanent deformation that occurred during the buckling tests.

5.4.3 During external pressurization of the barrel, data obtained for nitrogen and hydrogen gases respectively indicates coolant hole pressures of 92 and 91.6 psig and coolant hole flow rates of 0.032 and 0.00140 lb/min for a 100 psig external pressure. During internal pressurization of a coolant hole (no applied external pressure), permeability rates were obtained for the barrel at 100 psig of 0.002 lb/min for nitrogen gas and 0.000435 lb/min for hydrogen gas.

REFERENCES

1. "NRX-A Block I Mechanical Design" prepared by Mechanical Design, approved by A. Selz and W. G. Roman; Westinghouse Astronuclear Laboratory.

2. "Permeability of the Reimpregnated ND 215 Inner Reflector Cylinder - Data Analysis and Design Significance" prepared by A. Miller, approved by K. L. Rieke and J. G. Gallagher; WANL-TME-788, Westinghouse Astronuclear Laboratory.

3. "Theory of Elasticity", S. Timoshenko and J. N. Goodier, Engineering Societies Monographs; McGraw-Hill Book Co., Inc.; New York, New York.

4. "NRX-A1 Test Prediction" prepared by Reactor Analysis, approved by F. D. Retallick, WANL-TME-644, Westinghouse Astronuclear Laboratory.

5. "Reactor Analysis Data Book" prepared by Reactor Analysis, approved by J. G. Gallagher, WANL-TME-840, Westinghouse Astronuclear Laboratory.

6.0 APPENDIX A - Calculation of Stresses in Aluminum Shell and Graphite Inner Reflector Cylinder Due to Shrinkfit

6.1 Sample Calculation of Stress in Reflector Groove

Average O. D. of aluminum shell = 39.832 in. (measured)

Mean diameter of aluminum shell = 39.832 - .063 = 39.769 in. (nominal)

Average O. D. of graphite barrel = 39.7955 in. (measured)

Average groove I. D. of graphite barrel = 37.2449 in. (measured)

6.2 Stress in Aluminum Shell

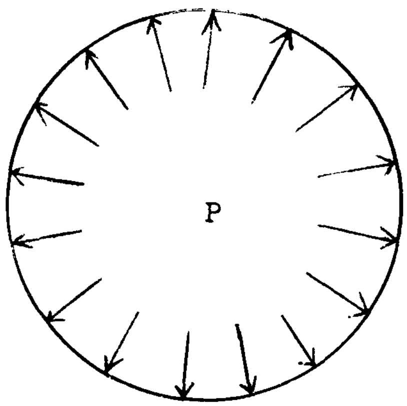

$$\sigma_a = \frac{P\ Da}{2\ t} = \frac{P \times 39.769}{2 \times .063}$$

$$\sigma_a = 315.625\ P$$

6.3 Stress in Graphite Barrel (at groove)

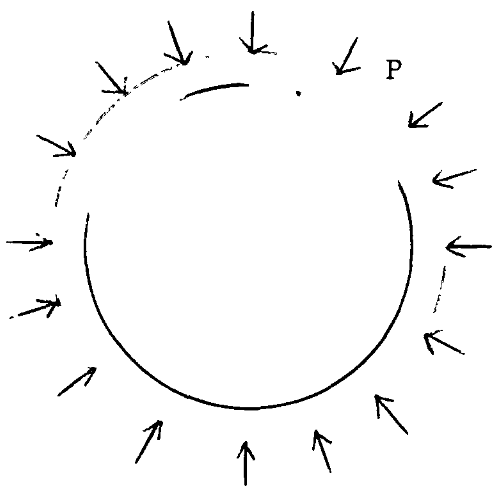

$$\sigma_g = \frac{D_o^2 + D_i^2}{D_o^2 - D_i^2}\ P$$

$$\sigma_g = \frac{(39.7955)^2 + (37.2449)^2}{(39.7955)^2 - (37.2449)^2}\ P$$

$$\sigma_g = -\ 15.119\ P$$

6.4 After Shrinking:

Inner Circumference of aluminum = outer circumference of graphite

$$(D_i)_a \pi + \frac{\sigma_a L_a}{E_a} = (D_o)_g \pi + \frac{\sigma_g L_g}{E_g}$$

$$(39.769 - .063) + \frac{39.769\,\sigma_a}{E_a} = 39.7955 + \frac{39.7955\,\sigma_g}{E_g}$$

Assume: $E_a = 10^7$; $E_g = 1.5 \times 10^6$

$$39.706 + 39.769 \times 10^{-7}\,\sigma_a = 39.7955 + 26.530 \times 10^{-6}\,\sigma_a$$

Substitute for σ_a and σ_g in terms of P

$$1255.209 \times 10^{-6} P + 401.107 \times 10^{-6} P = .0895$$

$$1656.316\ P = .0895 \times 10^6$$

$$\text{Pressure Equivalent} = P = 54.035\ \text{lb/in.}^2$$

Stress in aluminum shell:

$$\sigma_a = 316.571 \times 54.035 = 17{,}100\ \text{lb/in.}^2$$

Stress in graphite barrel (outside):

$$\sigma_g = -15.119 \times 54\ .035 = -817\ \text{lb/in.}^2$$

Stress in graphite barrel (inside):

$$\sigma_g = -\frac{2\,(D_o)^2}{D_o^2 - D_i^2}\,P = -\frac{2\,(39.7955)^2}{(39.7955)^2 - (37.2449)^2}\,P$$

$$\sigma_g = 16.119 \times 54.035 = -871\ \text{lb/in.}^2\ \text{(Compression)}$$

By similar calculations the stress on the land at station $4.624 = \sigma_g = -686$ lb/in.^{2} (Compression)

6.5 Pressure on Graphite Barrel Due to External Pressure on Aluminum Shell:

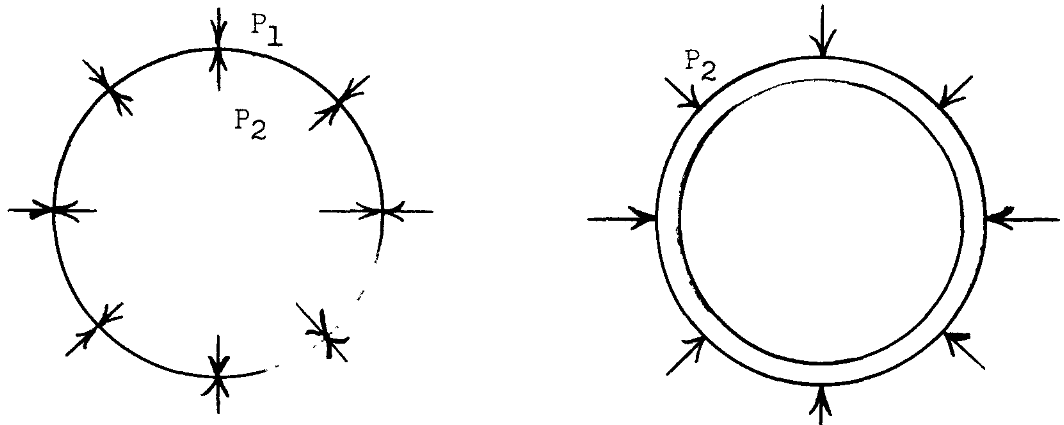

Aluminum Shell

Graphite Barrel

Δ diameter aluminum shell $= \Delta$ outer diameter of graphite barrel

$$\frac{(P_2 - 54.035 - P_1)\ (39.769)^2}{2 \times .063 \times 10^7} = - \frac{(P_2 - 54.035)\ (R_o^2 + R_i^2)\ (39.7955)}{(R_o^2 - R_i^2) \times 1.5 \times 10^6}$$

$$\frac{(39.769)^2\ P_2}{1.26} - \frac{54.035\ (39.769)^2}{1.26} - \frac{(39.769)^2\ P_1}{1.26}$$

$$= \frac{-15.119 \times 39.7955}{1.5} P_2 + \frac{15.119 \times 39.7955}{1.5} \times 54.035$$

$$1255.209\ P_2 - 67825.648 - 1255.209\ P_1 = 401.107\ P_2 + 21674.093$$

$$1656.316\ P_2 = 1255.209\ P_1 + 89499.741$$

$$P_2 - .758\ P_1 + 54.035$$

$$\therefore P_2 = .758 \times 0 + 54.035 = 54.035 \text{ lb/in.}^2 \ @\ P_1 = 0$$

$$P_2 = .758 \times 200 + 54.035 = 205.635 \text{ lb/in.}^2 \ @\ P_1 = 200 \text{ lb/in.}^2$$

6.5 Stress in Graphite Barrel (inner):

$$\sigma_g = 16.119 \text{ x } 54.035 = -871 \text{ lb/in.}^2 \text{ @ } P_1 = 0 \text{ lb/in.}^2$$

$$\sigma_g = 16.119 \text{ x } 205.635 = -3315 \text{ lb/in.}^2 \text{ @ } P_1 = 200 \text{ lb/in.}^2$$

Indicated strain in graphite (inner):

$$\epsilon_g = \frac{\sigma g}{E_g} = \frac{-871 -(-871)}{1.5 \text{ x } 10^{-6}} = 0 \, \mu \text{ in./in. @ } P_1 = 0 \text{ lb/in.}^2$$

$$\epsilon_g = \frac{-3315 - (-871)}{1.5 \text{ x } 10^{-6}} = -1629 \, \mu \text{ in./in. @ } P_1 = 200 \text{ lb/in.}^2$$

7.0 APPENDIX B - Procedure for Nitrogen and Hydrogen Permeability Tests of Inner Reflector Graphite Cylinder

7.1 Purpose:

7.1.1 The purpose of this test is to determine the nitrogen and hydrogen permeability rate of a production grade impregnated inner reflector graphite barrel.

7.2 Objectives:

7.2.1 The primary objective of this test is to determine the permeability rate of the inner reflector as a function of the pressure differentials across the thickness of the barrel. Permeability rate will be defined as the flow of gas necessary to maintain a constant pressure differential acorss the barrel thickness.

7.2.2 The strain induced in the graphite barrel at different circumferential and longitudinal positions around the inner periphery will be determined with respect to the nitrogen and hydrogen gas pressure.

7.2.3 The radial deflection of the reflector will be determined with respect to gas pressure, longitudinal position, and circumferential position.

7.3 Test Component

7.3.1 The test specimen will be a production grade inner reflector graphite cylinder. The part number is 936J568H04P.

7.4 Test Equipment

7.4.1 The inner reflector graphite cylinder will be inserted into a steel pressure vessel. Pressure differentials across the barrel will be supplied with nitrogen and hydrogen gas flowing between the steel vessel and the graphite barrel. Figure 22 shows the test pressure vessel and associated equipment for applying and measuring the gas pressure. Strain gage readings were recorded using Baldwin-Lima Hamilton strain indicators and switching units. Barrel deflections were recorded using linear variable differential transformers (LVDT's) and Endevco recording equipment

7.5 Test Sequence

7.5.1 Install rubber plugs in all plunger holes of the inner reflector cylinder.

7.5.2 Install strain gages and LVDT's on the graphite barrel as shown in Figures 23. Insert the barrel into the steel pressure vessel and preload the tie down bolts to 800 micro-inches strain. Connect up tubing to test pressure vessel, flowmeter, manifold, etc. as shown in Figure 22.

7.5.3 Prior to the start of the test, check the pressure on each nitrogen and hydrogen gas supply to insure full tanks (2000 psi or better).

7.5.4 Apply nitrogen gas pressure to the barrel up to 20 psi for purge and checkout of the system. Apply leak-tec to the interior of the graphite barrel and system to insure gastight conditions.

7.5.5 Apply nitrogen gas pressure to the barrel and hold at 10, 30, 50, 60, 70, 80, 90, and 100 psig for strain readings. Record the flowmeter readings, flowmeter inlet pressure, and flowmeter inlet temperature manually. Readings must be taken as quickly as possible. Pressure and deflection readings will be recorded continuously during testing. Also, strain gages installed according to Figure 23 should be continuously recorded. At the completion of data acquisition at 100 psig, reduce the pressure to 60 psig and 30 psig and repeat all readings.

7.5.6 Turn off the nitrogen gas after completing all readings at 30 psig. Repeat item 7.5.4 of this procedure.

7.5.7 Turn off the nitrogen gas and turn on hydrogen gas. Repeat item 7.5.5.

7.5.8 Turn off hydrogen gas and turn on nitrogen gas (20 psig) for purging the system.

7.5.9 Test completed.

7.6 Test Parameters

7.6.1 The inner reflector permeability tests were performed under the following conditions:

7.6.1.1 Ambient Temperature

7.6.1.2 Differential Pressure - 0 to 100 psig

7.7.1.3 Nitrogen and Hydrogen Gas Environment

8.0 APPENDIX C - Procedure for Accumulating Axial Cooling Hole Porous Flow Data for Inner Reflector Graphite Cylinder

8.1 Purpose:

8.1.1 The purpose of this test is to determine the pressure level and gas flow rate in the cooling holes of the inner reflector barrel. These measurements were obtained during external pressurization of the barrel and during internal pressurization of a cooling hole.

8.2 Test Objectives:

8.2.1 Determination of the pressure level and gas flow rate in a reflector peripheral cooling hole during external pressurization of the barrel.

8.2.2 Determination of the permeability rate of the barrel during internal pressurization of a cooling hole (zero external pressure).

8.3 Test Component

8.3.1 The test component will be the inner reflector graphite cylinder, part number 936J568H04P.

8.4 Test Equipment

8.4.1 The inner reflector barrel was inserted into a steel pressure vessel. External pressurization of the barrel was supplied from nitrogen and hydrogen gas flowing between the barrel and the test vessel. Figure 22 shows the test pressure vessel and associated equipment for applying and measuring the gas pressure.

8.4.2 Internal pressurization of the reflector cooling hole was accomplished using the modified test assembly shown in Figure 24 in conjunction with the above. Pressure and flow rate in the cooling tube were determined using a Heise pressure gage and Fisher-Porter Flowmeter (Figure 25).

8.5 <u>Test Sequence</u>

8.5.1 Prior to inserting the inner reflector into the steel pressure vessel, one of the cooling holes at the nozzle end of the reflector should be plugged such that no gas flow can enter or leave the hole at this position. Accurate measurements must be obtained for the diameter of the cooling hole, the length of the hole from the end of the plug section, and the length and diameter of tubing from the dome end to the Heise pressure gage (Figure 24).

8.5.2 After inserting the barrel into the steel vessel and sealing the dome end with silastic (gastight seal required), the nozzle end should be set in silastic before attaching the aluminum flange. Installation of tubing, etc., into the cooling hole should be done according to Figure 24.

8.5.3 Prior to the start of testing, all tubing connections, reflector plugs, and seals should be checked for leakage using leak-tek. Pressure levels on all gas supply bottles should be at least 2000 psi. The tie bolts (controlling reflector axial load) should be preloaded to 800 μ in./in. strain (approximately 16,900 lb).

8.5.4 The first test will consist of externally pressurizing the inner reflector. Gas pressure will be applied to the external surface of the barrel in steps of 0, 10, 20, 30, 40, 50, 60, 70, 80, 90 and 100 psig. Gas flow rate, flowmeter pressure, etc. (with respect to pressurizing the surface of the barrel), will be recorded at each pressure level (Figure 22), At each pressure level the following procedure will be followed to obtain cooling hole pressure and flow rate data (Figure 25).

8.5.4.1 Shut off valves 1 and 2 and record the pressure reading on the Heise gage.

8.5.4.2 Shut off valve 2 and open valves 1 and 3 and record the Heise pressure reading, and flowmeter reading.

After completion of the readings at 100 psig, the external pressure will be reduced in steps of 10 psig and all the above readings repeated. Note that care should be taken in order that all readings are obtained when the pressure at each level is stabilized.

8.5.5 The second test will consist of internally pressurizing a cooling hole of the inner reflector. No external pressure will be applied to the surface of the barrel during this test (Figure 22). Valves 1 and 3 will be closed during testing. Gas pressure will be applied by opening valves 2 and 4. Pressure will be applied in steps of 0, 10, 20, 30, 40, 50, 60, 70, 80, 90 and 100 psig. At each pressure level, pressure gages 1 and 2 (Figure 25) and flowmeter readings will be recorded. After obtaining readings at 100 psig, gas pressure will be reduced in steps of 10 psig and all readings repeated. One again, care should be taken so that pressure levels are stabilized prior to taking readings.

8.5.6 The preceding tests will be performed under nitrogen and hydrogen gas environments. It should be noted that when using hydrogen gas, the system must be purged with nitrogen gas at 20 psig pressure before and after each test.

8.6 <u>Test Parameters</u>

8.6.1 The reflector cooling hole tests will be performed under the following conditions:

8.6.1.1 Ambient Temperature

8.6.1.2 Gas Pressure Levels of 0 to 100 psig.

8.6.1.3 Nitrogen and Hydrogen Gas Environments.

9.0 APPENDIX D - Buckling Test of the Inner Reflector - Procedure for Determining the Structural Integrity of the Inner Reflector

9.1 Purpose:

9.1.1 The complete geometrical configuration of the inner reflector severely hampers any accurate detailed design analysis. Therefore, in order to substantiate the structural integrity of the reflector for NRX-A1 (NRX-A2) test conditions, a series of experimental investigations are required.

9.2 Test Objectives:

9.2.1 The structural integrity of the inner reflector under NRX-A1 (NRX-A2) operating conditions will be determined.

9.2.2 A relationship between the NRX-A1 pressure profile, reflector strains and deflections will be determined.

9.2.3 The critical buckling pressure and buckling mode, if occurring within NRX-A1 operating conditions, will be determined.

9.2.4 The reflector will be inspected before and after the test series to determine any permanent deformation resulting from the pressure load.

9.3 Test Specimen:

9.3.1 The test component will be the inner reflector graphite cylinder (Part No. 936J568H04P). An aluminum barrel (.060 in. thick) will be used to simulate the core support barrel in the reactor.

9.4 Test Equipment

9.4.1 The inner reflector (having the simulated aluminum core support barrel encompassing the periphery) will be placed in a steel pressure vessel (Figure 21). This test vessel is equipped with seal chambers that allowed ramp pressurization of the reflector and encompassing aluminum barrel. Strain gages and linear variable displacement transducers, mounted on the inner periphery of the reflector, were recorded on a Baldinw-Lima Hamilton Strain Indicator and Endevco continuous recording equipment.

9.5 Test Sequence

9.5.1 The simulated aluminum core support barrel was heated to 400°F in order to allow sufficient clearance for the aluminum to slide freely over the inner reflector. Upon returning to room temperature, the aluminum barrel will shrink onto the graphite cylinder inducing compressive strains in the reflector. These strains will be monitored on the inner periphery of the reflector. Strain gages and linear variable displacement transducers will be installed on the inner periphery of the reflector as shown in Figure 23.

9.5.2 The inner reflector and encompassing aluminum barrel will then be placed in a steel pressure vessel. Surfaces of the reflector mating with the steel pressure vessel will be sealed with silastic to prevent any gas leakage. An axial load will be imparted to the reflector by tightening a series of tie bolts (surounding the inner periphery of the cylinder and interconnecting the test vessel) to 800μin./in. strain.

9.5.3 The reflector and aluminum barrel will be subjected to an environment of nitrogen gas. The gas will be supplied in ramp fashion along the length of the barrel using the apparatus described in Figure 26. Pressure profiles simulating NRX-A1 and NRX-A2 operating conditions will be used (Figure 27). Also, an attempt will be made to simulate NRX-A3 full power operating conditions represented in Figure 28. The gas pressure to be supplied in each chamber of the test vessel is described in steps on these figures. At each step, strain readings and deflection readings will be recorded. At completion of the maximum pressure reading for each condition, the pressure will be reduced in similar steps and all readings repeated until 0 psig is reached.

9.6 <u>Test Parameters</u>

9.6.1 Ambient Temperature

9.6.2 Nitrogen Gas Environment

9.6.3 Ramp Pressure to a Maximum of 175 psig.

10.0 APPENDIX E - Dimensional History of Inner Reflector Cylinder

Outer Diameter of Reflector (Inches)

	Station 6.030				Station 28.566				Station 48.250			
	LOCATION				LOCATION				LOCATION			
	0°	45°	90°	135°	0°	45°	90°	135°	0°	45°	90°	135°
Vendors Data	Range 39.793 to 39.798				Range 39.793 to 39.798				Range 39.793 to 39.798			
Before Re-impregnation	39.7955	39.7975	39.7985	39.7950	39.790	39.791	39.791	39.791	39.799	39.7965	39.797	39.796
Before Testing to 200 psig	39.798	39.798	39.796	39.798	39.794	39.794	39.793	39.791	39.795	39.799	39.800	39.790
After Testing to 200 psig	39.746	39.836	39.815	39.712	39.746	39.834	39.802	39.707	39.741	39.826	39.802	39.708

Inner Diameter of Reflector (Inches)

	Station 6.030				Station 28.566				Station 48.250			
	LOCATION				LOCATION				LOCATION			
	0°	45°	90°	135°	0°	45°	90°	135°	0°	45°	90°	135°
Vendors Data	Range 37.246 to 37.253				Range 37.246 to 37.253				Range 37.246 to 37.253			
Before Re-impregnation	37.2425	37.2475	37.2465	37.2410	37.2435	37.2445	37.246	37.244	37.245	37.241	37.246	37.249
Before Testing to 200 psig	37.2465	37.247	37.244	37.2445	37.2430	37.247	37.248	37.244	37.241	37.244	37.249	37.241
After Testing to 200 psig	37.2960	37.2850	37.2760	37.1530	37.2210	37.289	37.195	37.142	37.205	37.272	37.228	37.155

WALL THICKNESS
(Inches)

	Reactor End				Nozzle End			
	LOCATION				LOCATION			
	0°	45°	90°	135°	0°	45°	90°	135°
Vendors Data	None Given				None Given			
Before Reimpregnation	1.839	1.840	1.839	1.838	1.838	1.840	1.840	1.834
Before Testing to 200 psig	1.844	1.840	1.840	1.840	1.844	1.840	1.840	1.840
After Testing to 200 psig	1.840	1.839	1.840	1.838	1.838	1.840	1.838	1.839

REFLECTOR HEIGHT

	LOCATION			
	0°	45°	90°	135°
Vendors Data	53.368 (one reading given)			
Before Reimpregnation	53.3645	53.363	53.364	53.365
Before Testing to 200 psig	53.3670	53.369	53.369	53.367
After Testing to 200 psig	53.3690	53.369	53.368	53.367

CONFIDENTIAL
RESTRICTED DATA
Atomic Energy Act - 1954

Astronuclear

WANL-TME-768

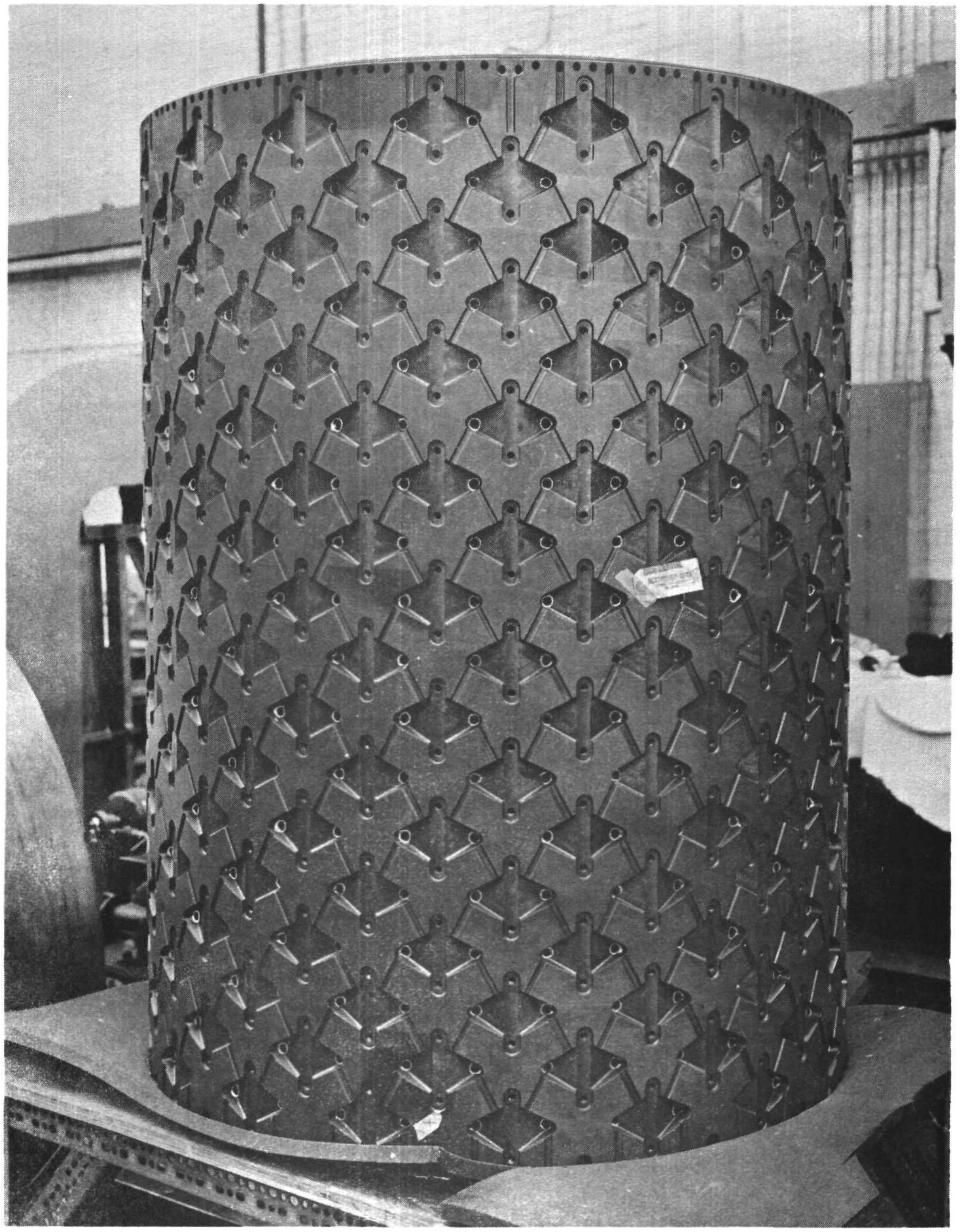

Figure 1

Inner Reflector Graphite Cylinder
(Part No. 936J568H04P)

CONFIDENTIAL
RESTRICTED DATA
Atomic Energy Act - 1954

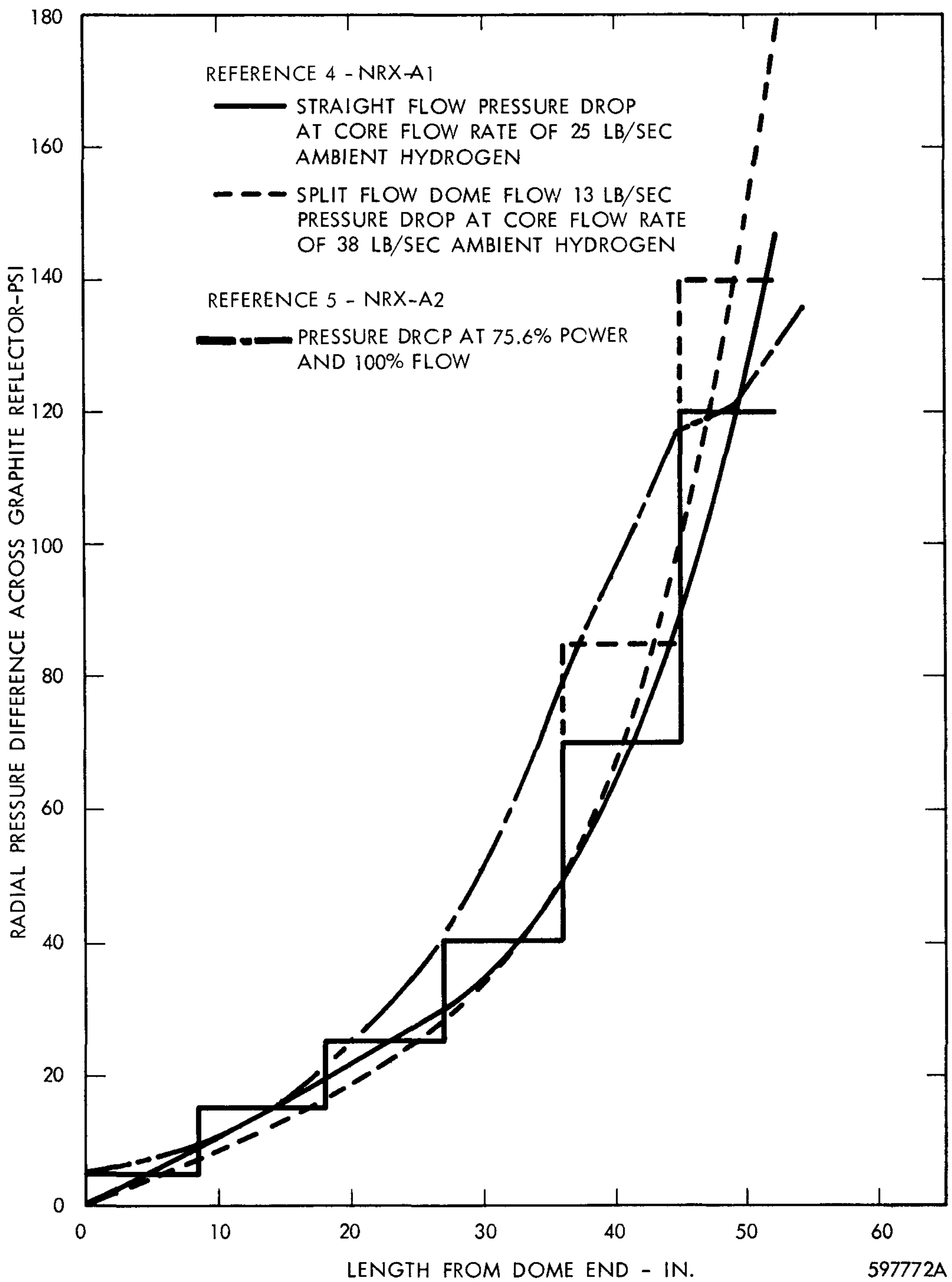

RAMP SIMULATION OF NRX-A1 PRESSURE PROFILE

Figure 2

CONFIDENTIAL
RESTRICTED DATA
Atomic Energy Act - 1954

Astronuclear

WANL-TME-768

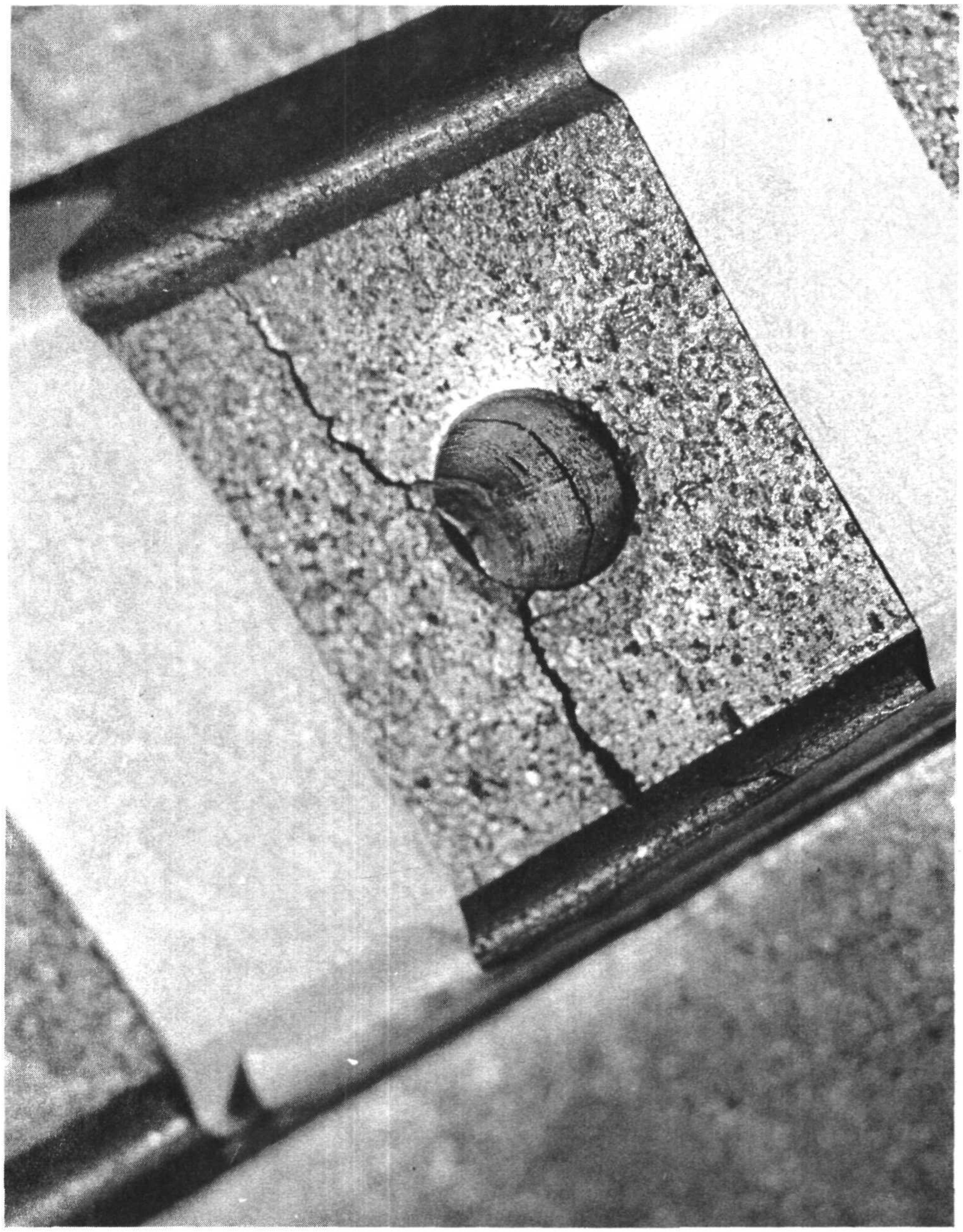

Figure 3
Cracked Area of Inner Reflector
(Third Lateral Support Seal Segment Groove from Reflector Dome End)

CONFIDENTIAL
RESTRICTED DATA
Atomic Energy Act - 1954

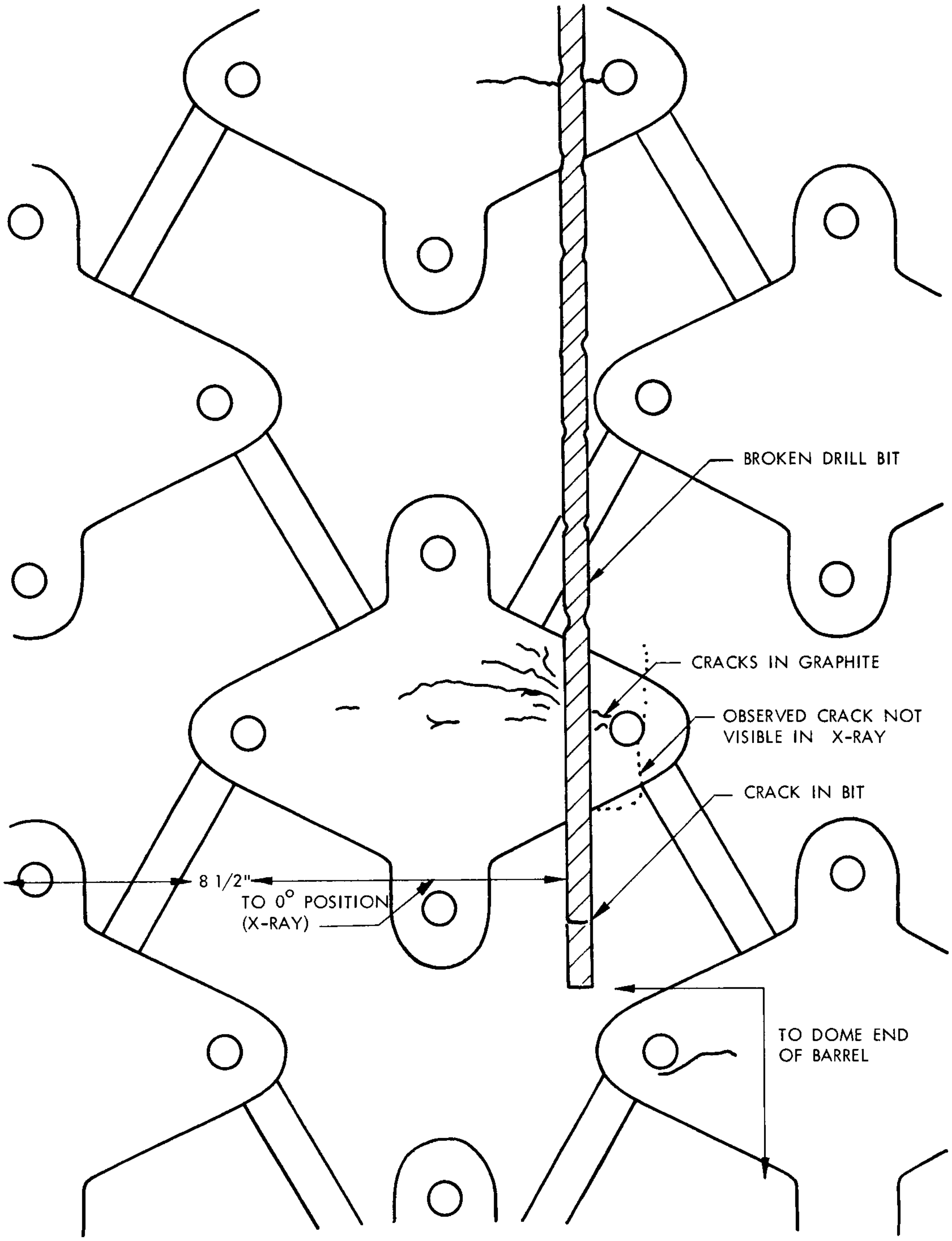

X-RAY REPRINT OF REFLECTOR CRACKED AREA 601815B

Figure 4

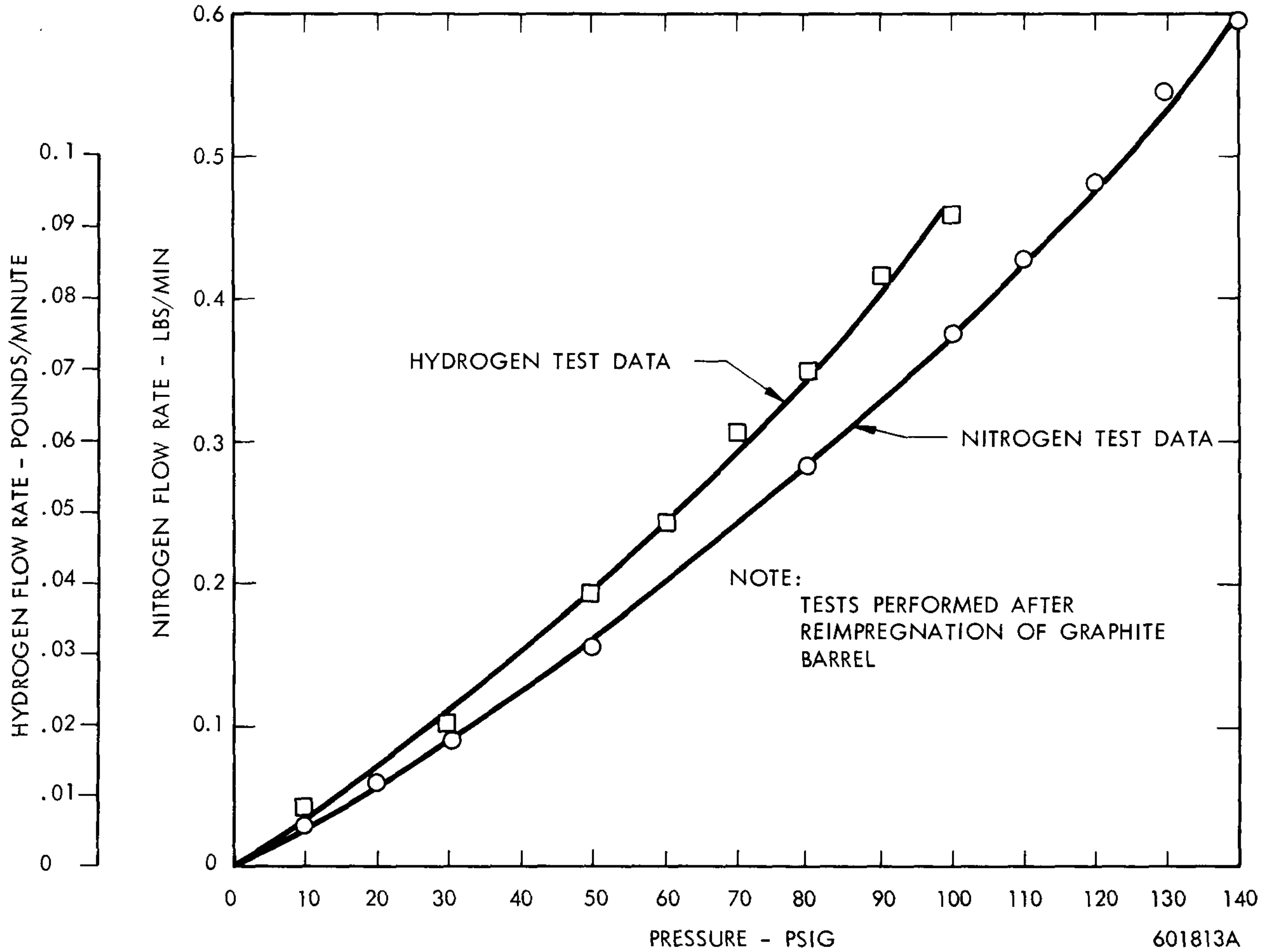

PERMEABILITY TEST OF INNER REFLECTOR GRAPHITE BARREL

Figure 5

~~CONFIDENTIAL~~
~~RESTRICTED DATA~~

Figure 6

~~CONFIDENTIAL~~
~~RESTRICTED DATA~~
Atomic Energy Act

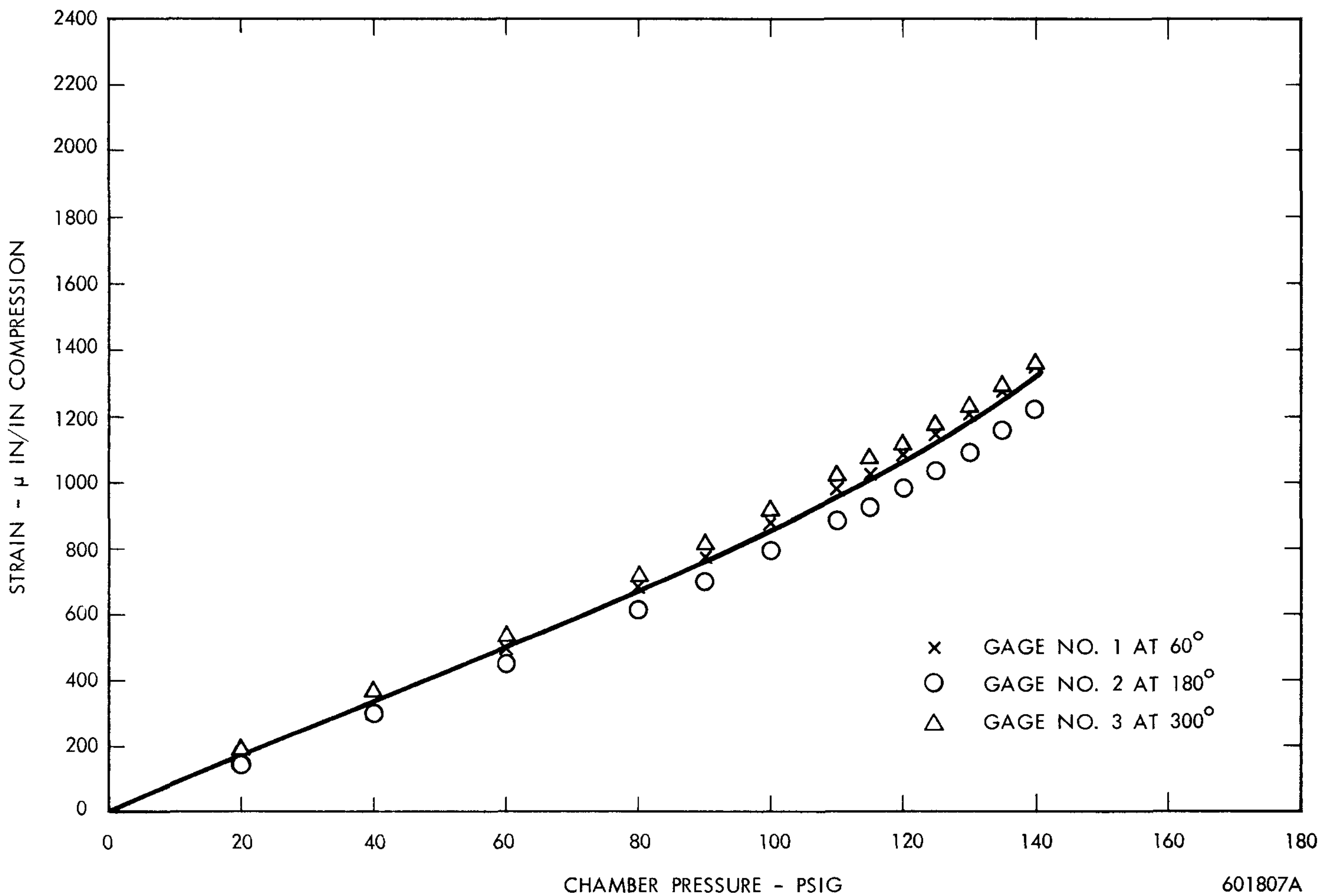

601807A

INNER REFLECTOR BUCKLING TEST, STRAIN VERSUS CHAMBER PRESSURE STA. 4.624 (LAND), CIRCUMFERENTIAL COMPRESSION

Astronuclear

[redacted] ~~RESTRICTED DATA~~ [redacted]

Figure 7

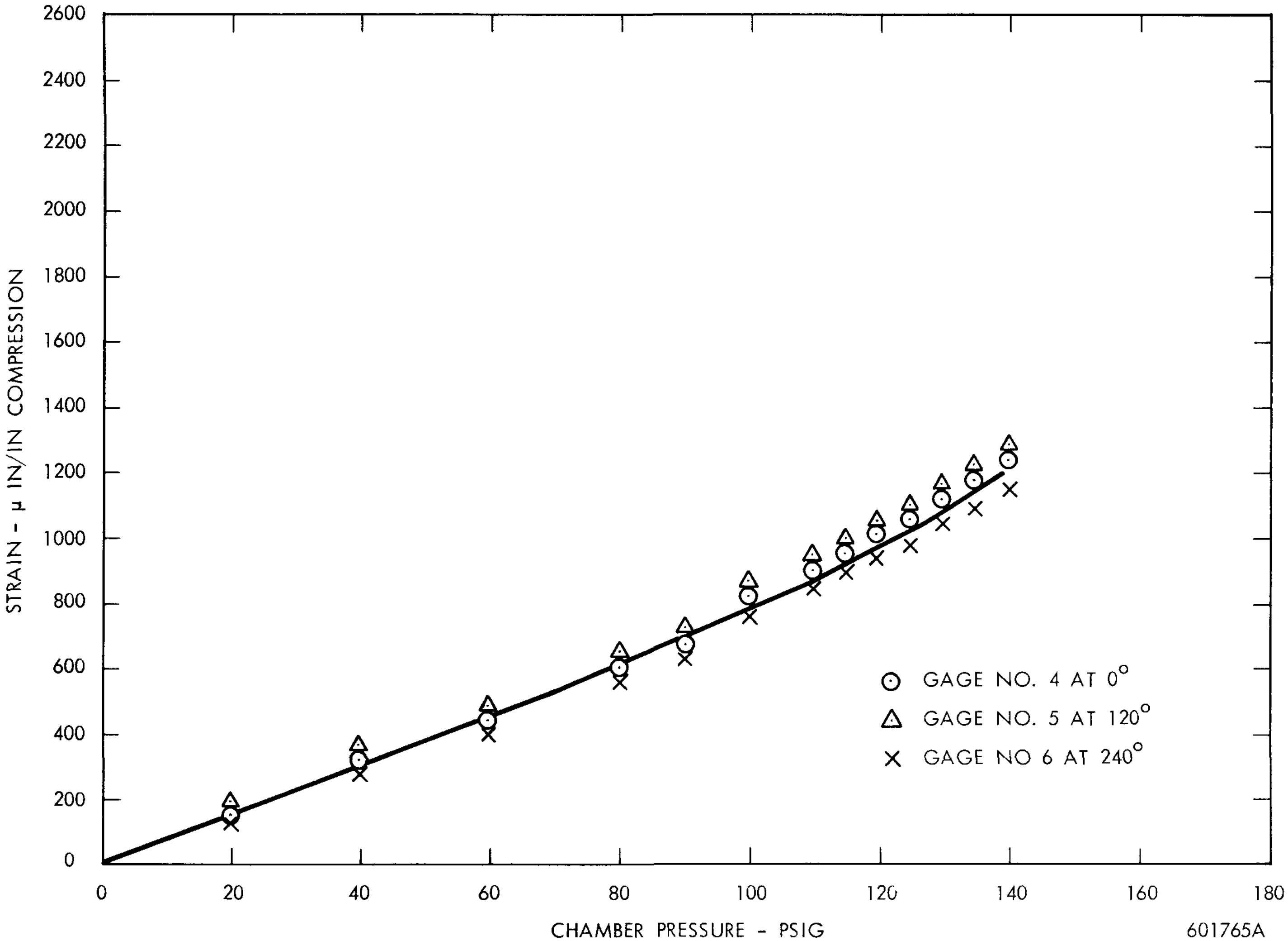

INNER REFLECTOR BUCKLING TEST, STRAIN VERSUS CHAMBER PRESSURE STA. 6.030 (GROOVE), CIRCUMFERENTIAL COMPRESSION

[redacted] ~~RESTRICTED DATA~~ [redacted]

WANL-TME-768

Astronuclear

CONFIDENTIAL
[redacted]

Figure 8

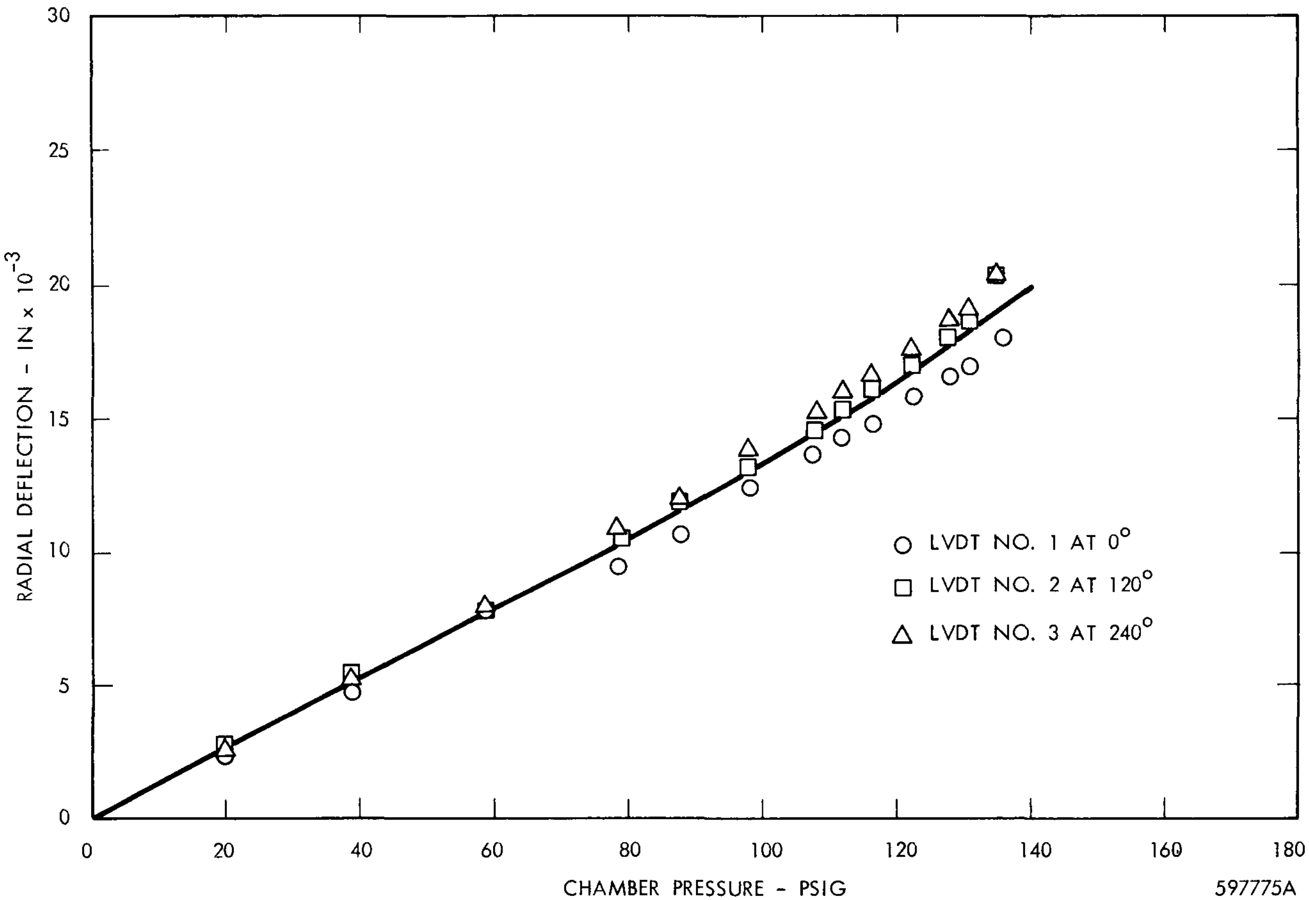

INNER REFLECTOR BUCKLING TEST, RADIAL DEFLECTION VERSUS CHAMBER PRESSURE

CONFIDENTIAL
[redacted]

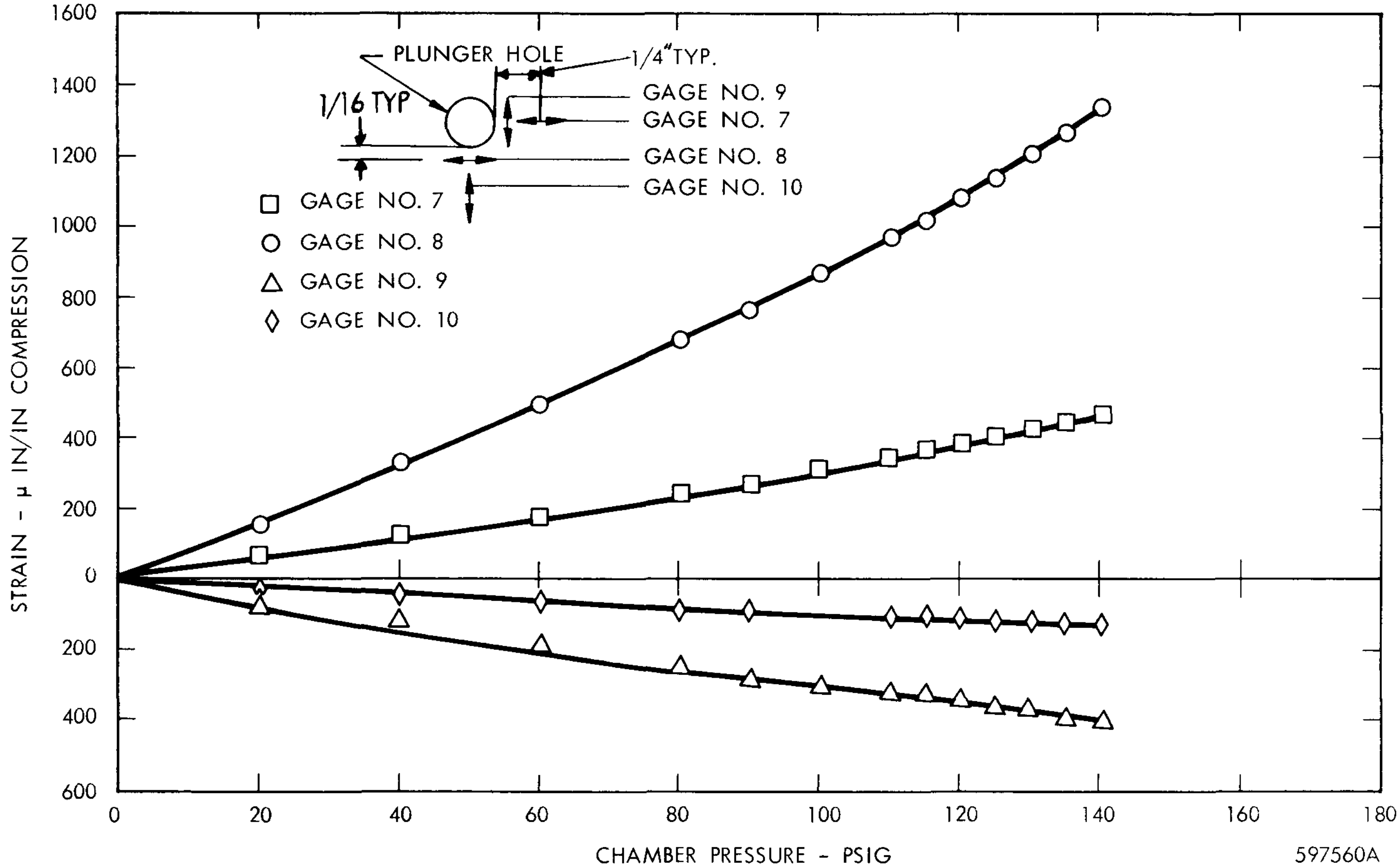

INNER REFLECTOR BUCKLING TEST, STRAIN VERSUS CHAMBER PRESSURE PLUNGER HOLE STA. 6.030 - 175°

Figure 9

WANL-TME-768

Astronuclear

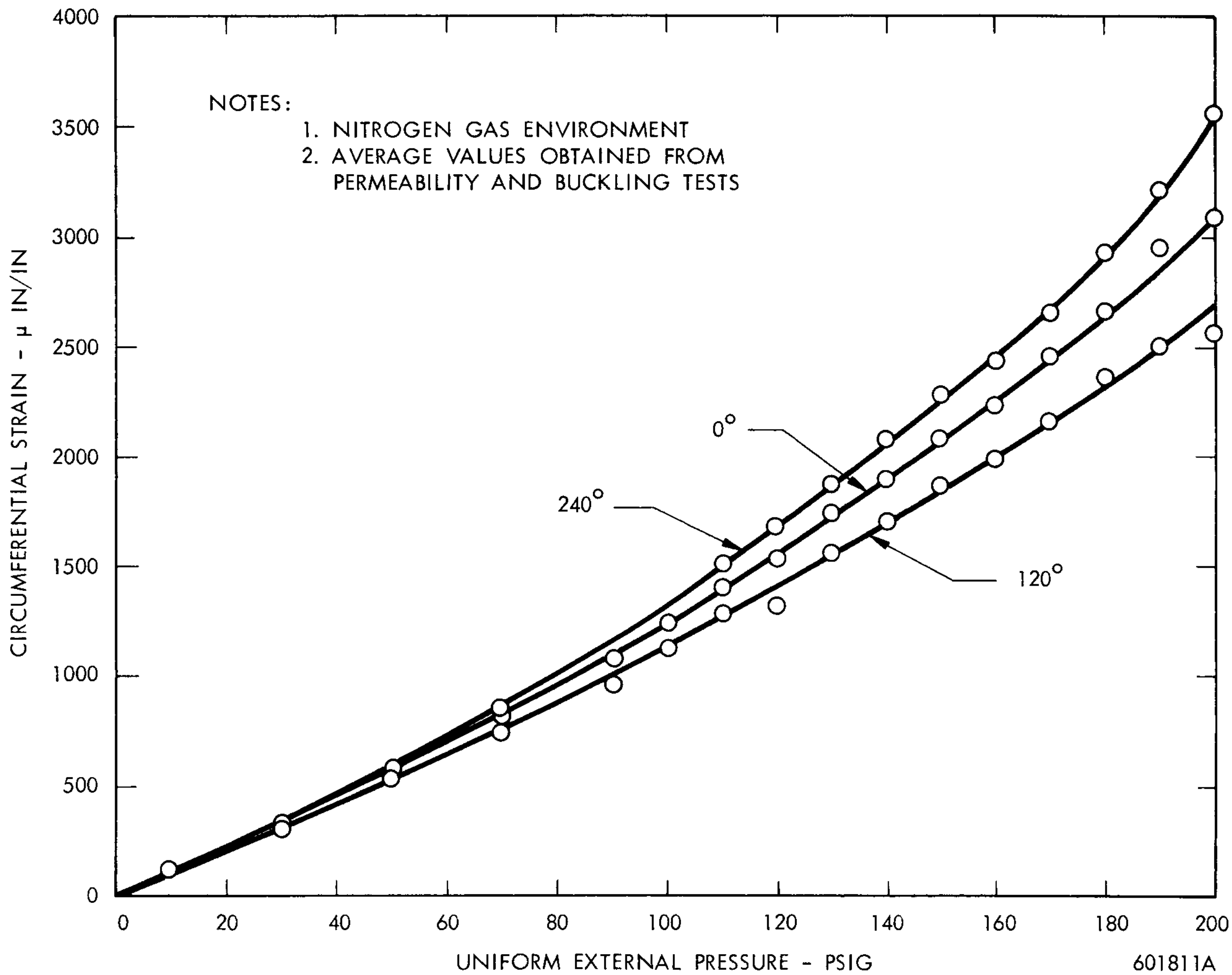

BUCKLING TEST OF INNER REFLECTOR GRAPHITE CYLINDER, PRESSURE VERSUS CIRCUMFERENTIAL STRAIN AT DIFFERENT CIRCUMFERENTIAL POSITIONS (STA. 28.566)

Figure 10

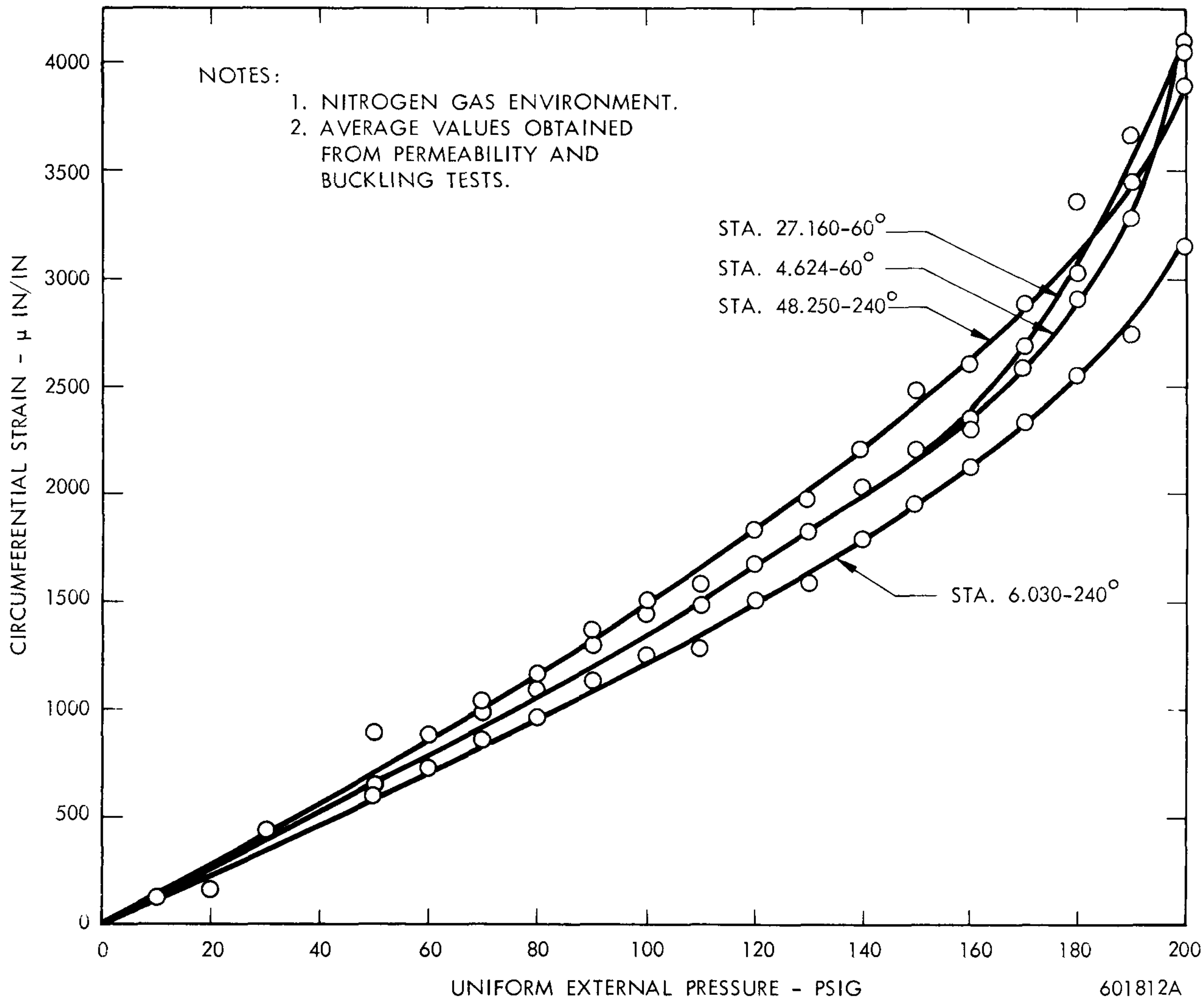

BUCKLING TEST OF INNER REFLECTOR GRAPHITE CYLINDER, PRESSURE VERSUS CIRCUMFERENTIAL STRAIN AT DIFFERENT AXIAL POSITIONS

Figure 11

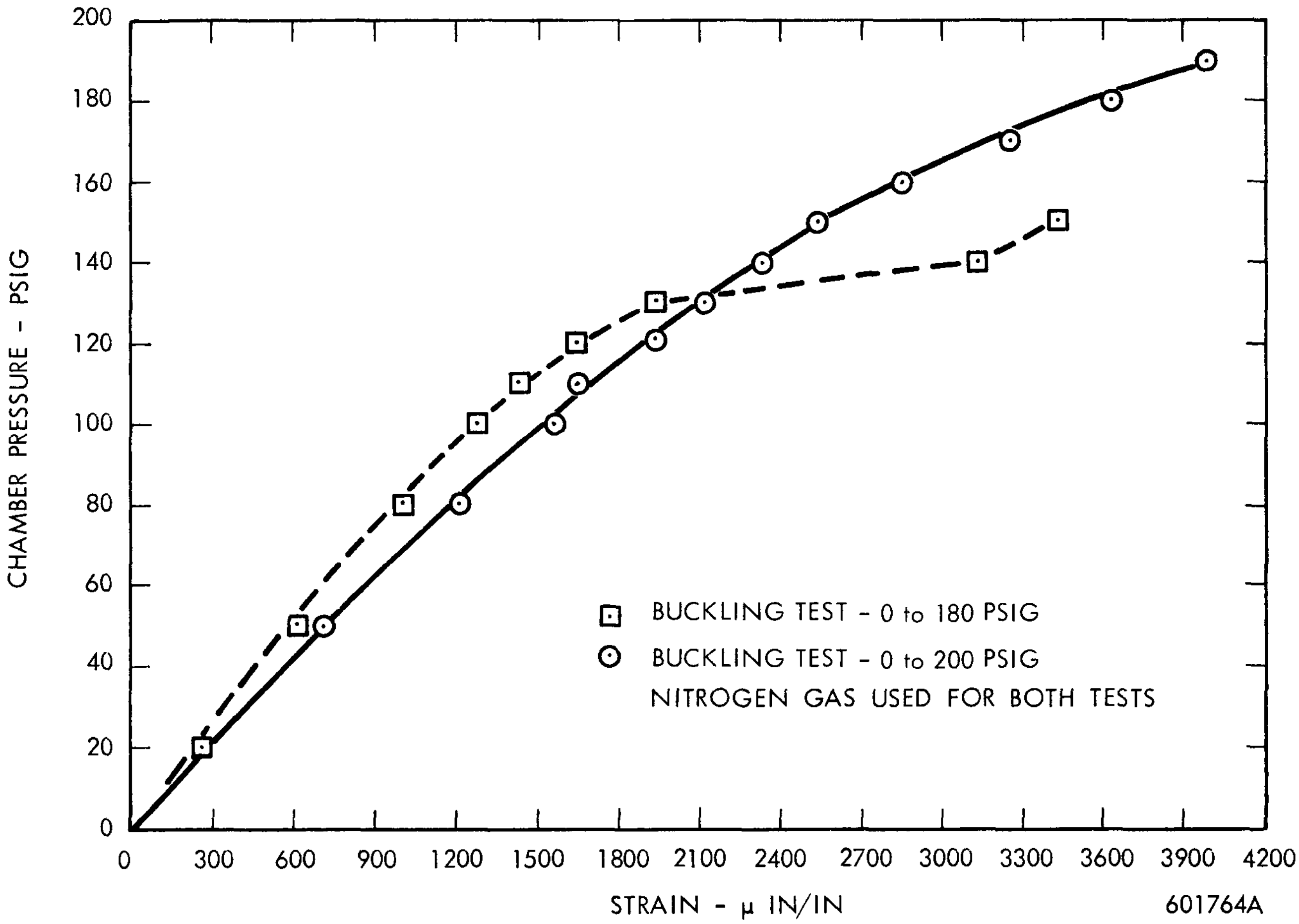

BUCKLING TEST OF INNER REFLECTOR BARREL, CHAMBER PRESSURE VERSUS STRAIN (CRACKED AREA - STA. 45.483)

Figure 12

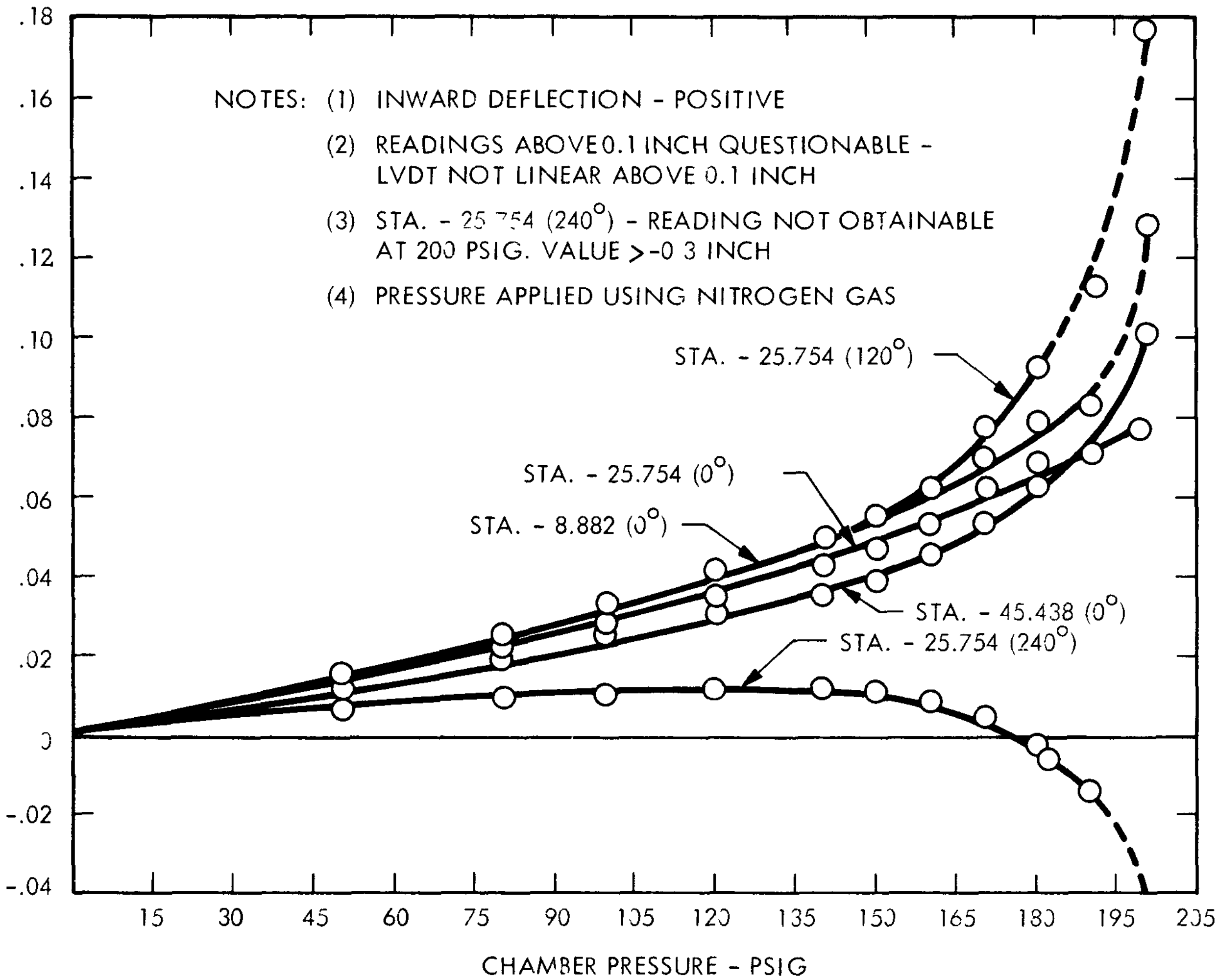

597767A

BUCKLING TEST OF INNER REFLECTOR BARREL, CHAMBER PRESSURE VERSUS RADIAL DEFLECTION

Figure 13

STRESS-STRAIN CHARACTERISTICS OF IMPREGNATED
H4LM GRAPHITE COMPRESSION - TANGENTIAL ORIENTATION

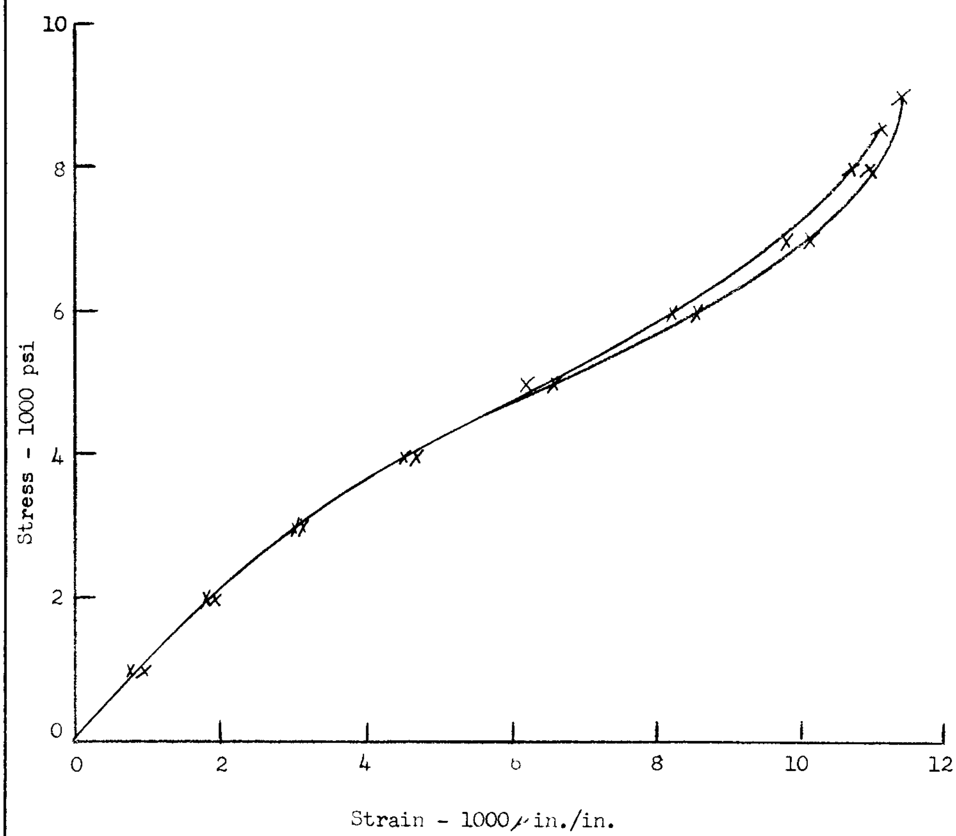

Materials
A. Pollack

Notes: (1) Specimen impregnated with silca dioxide
(2) Tests performed by WANL Materials Department

Figure 14

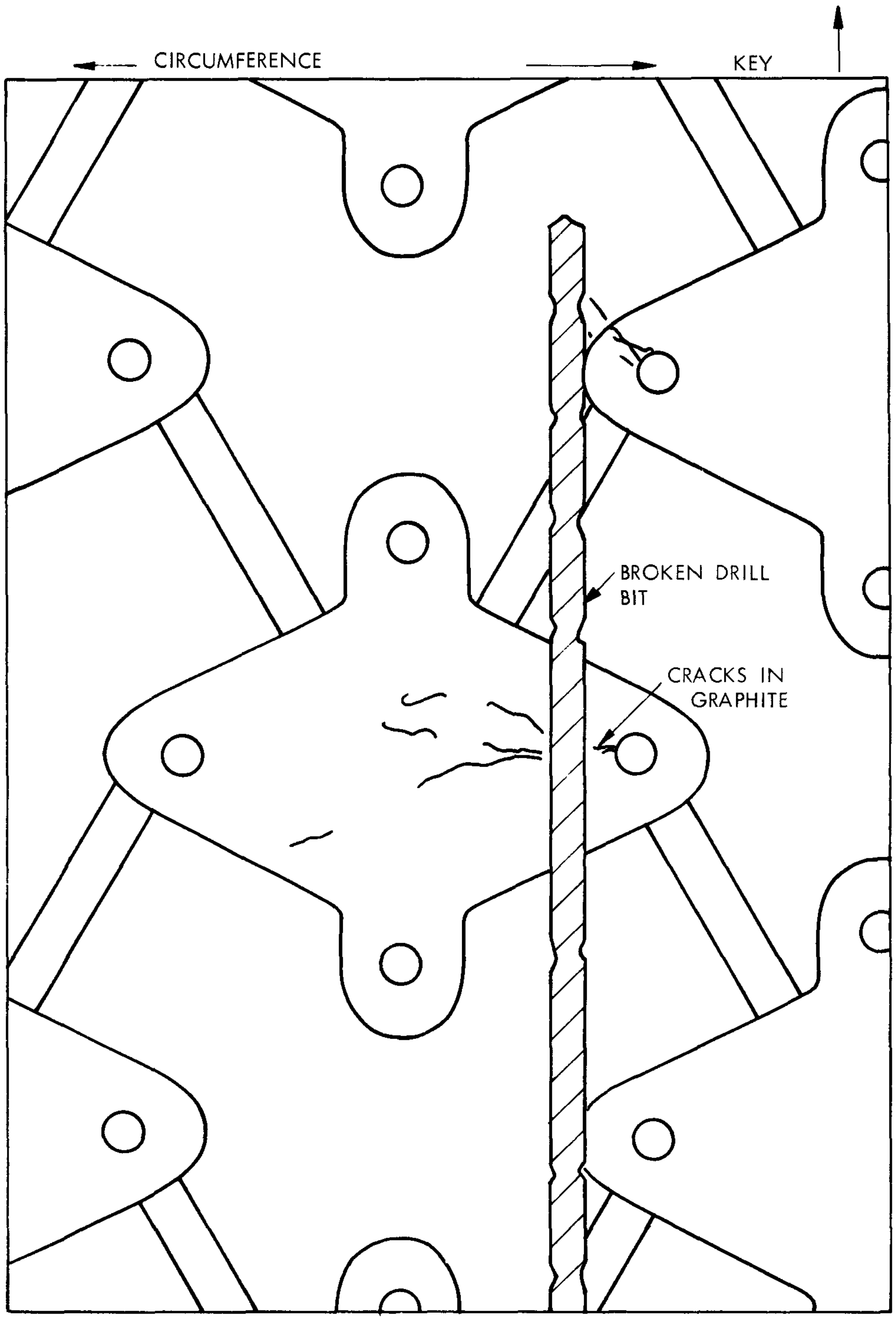

X-RAY OF CRACKED AREA AFTER RAMP PRESSURIZATION TESTS 601814B

Figure 15

~~CONFIDENTIAL~~
~~RESTRICTED DATA~~

Figure 16

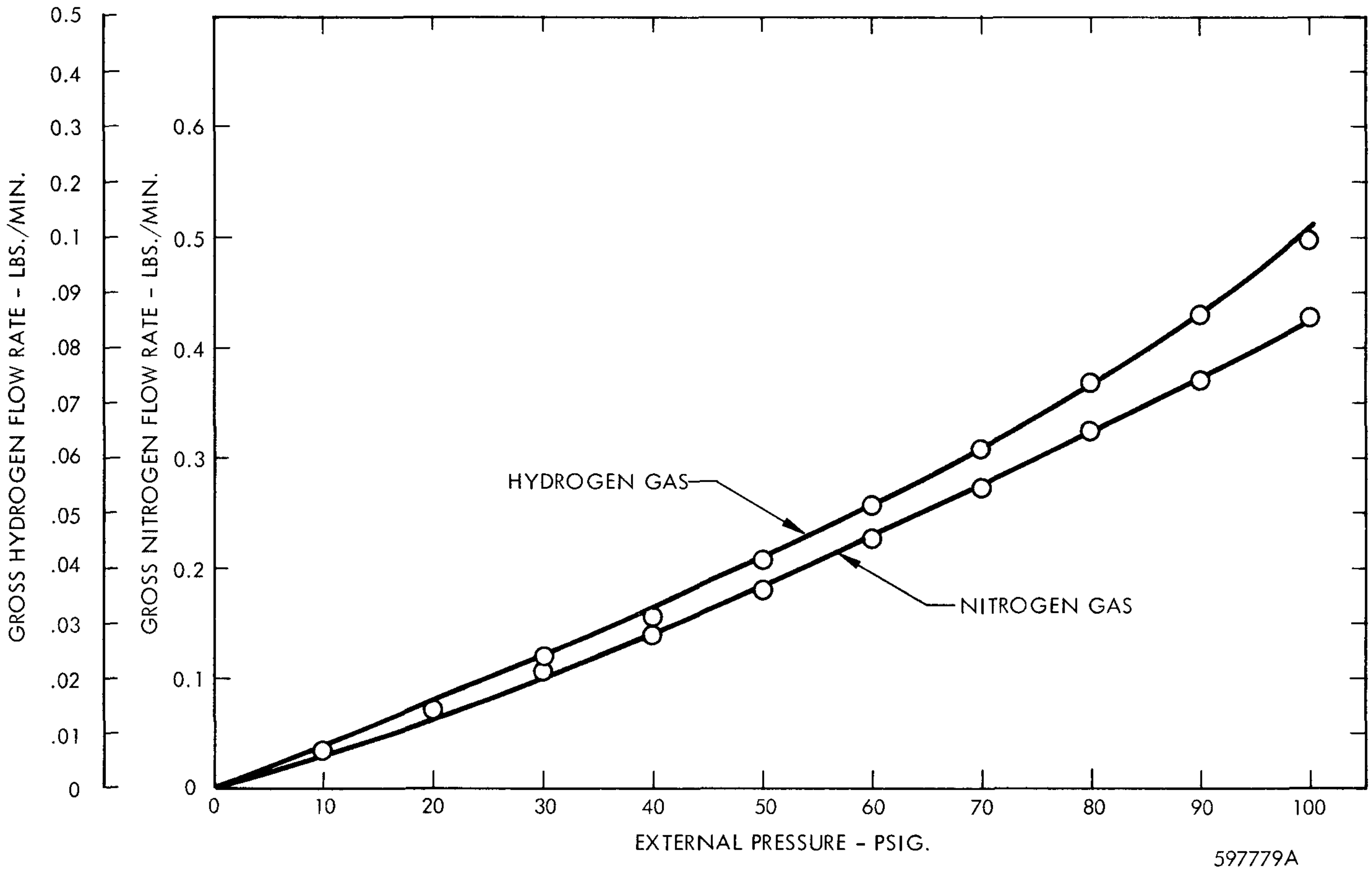

INNER REFLECTOR COOLANT HOLE POROUS FLOW TEST

INNER REFLECTOR GROSS FLOW RATE

~~CONFIDENTIAL~~
~~RESTRICTED DATA~~
~~Atomic Energy Act 1954~~

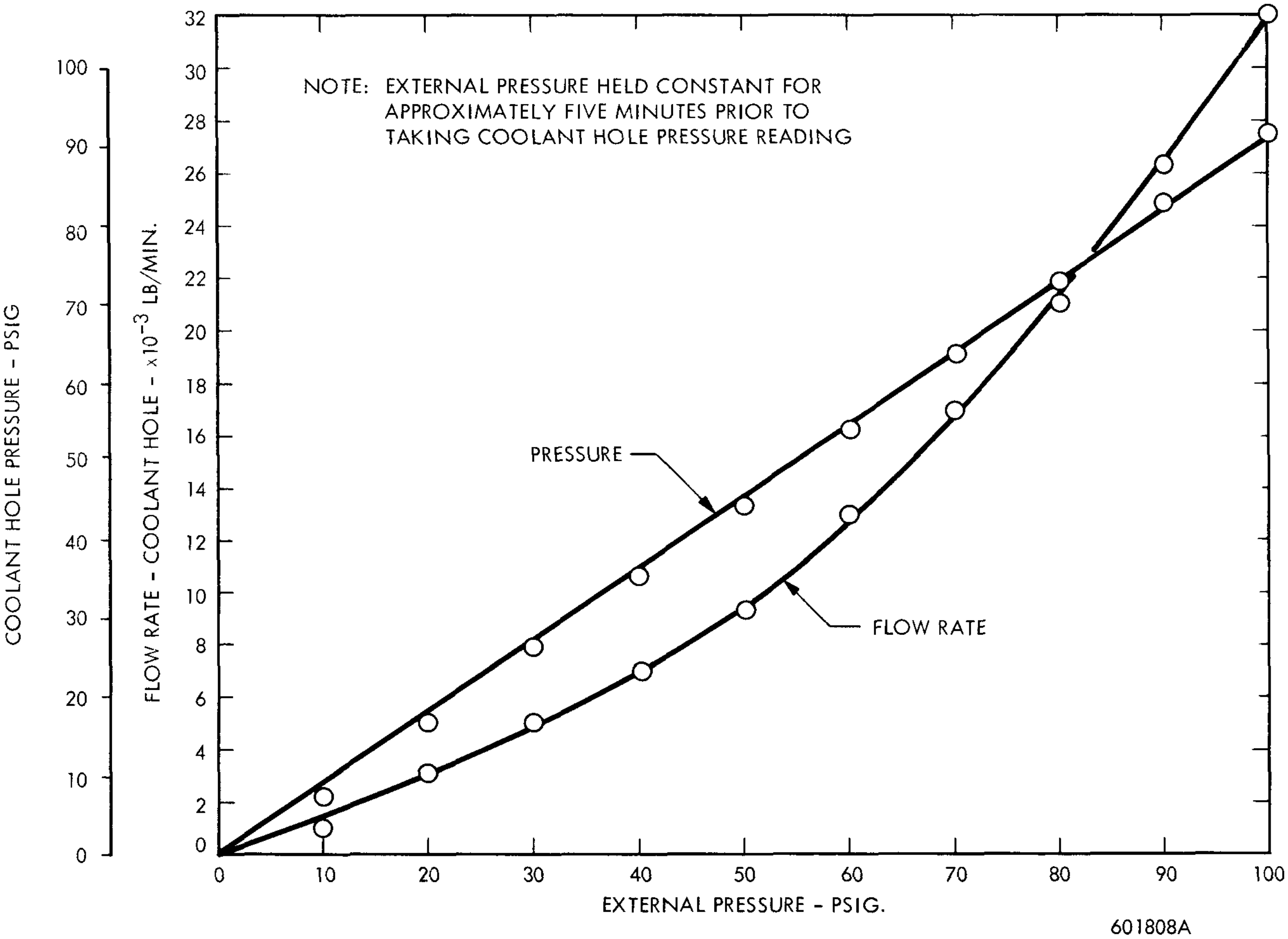

INNER REFLECTOR COOLANT HOLE POROUS FLOW TEST, EXTERNAL PRESSURIZATION OF INNER REFLECTOR NITROGEN GAS ENVIRONMENT

Figure 17

[redacted]

Figure 18

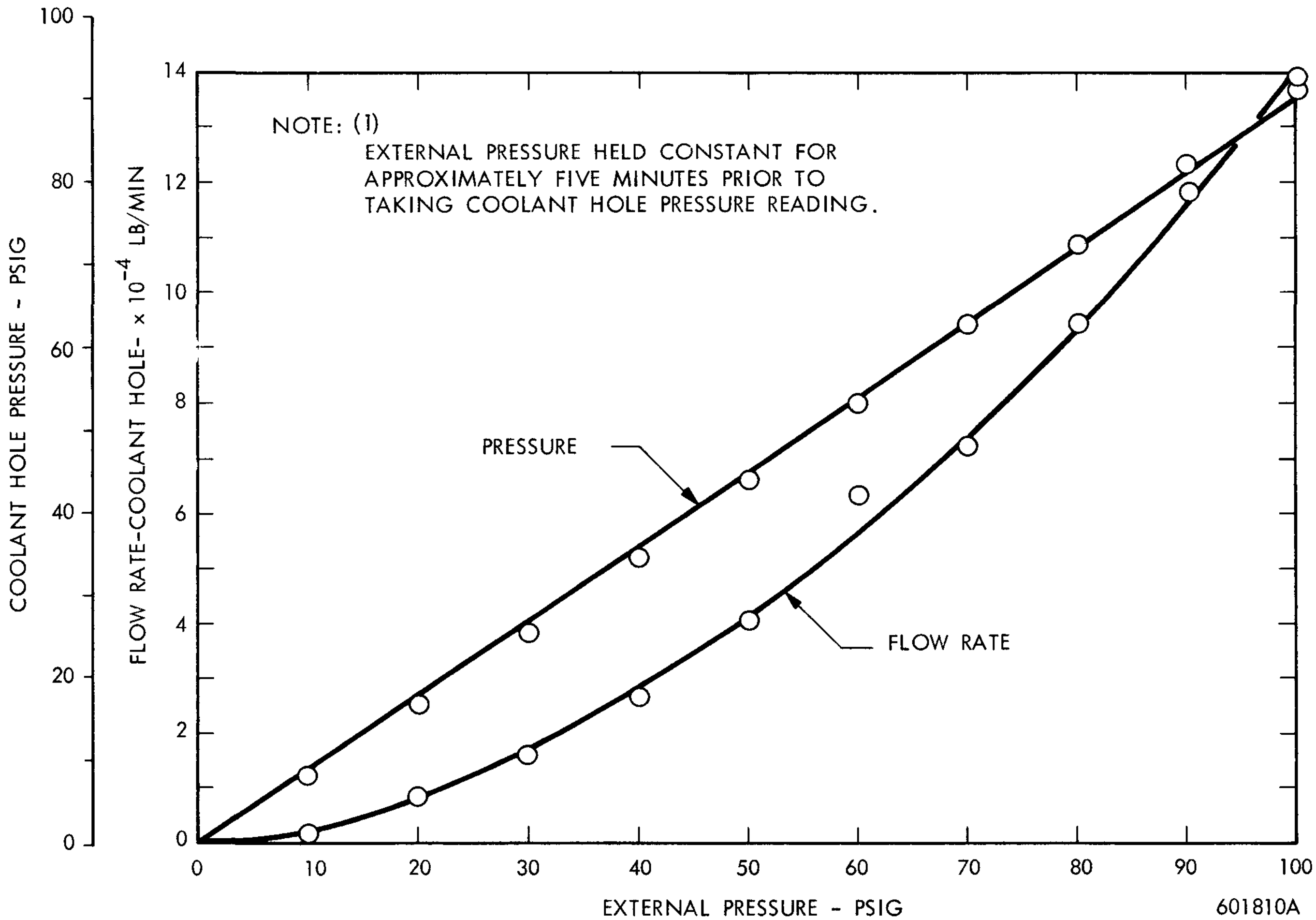

INNER REFLECTOR COOLANT HOLE POROUS FLOW TEST, EXTERNAL PRESSURIZATION OF INNER REFLECTOR, HYDROGEN GAS ENVIRONMENT

[redacted] ~~RESTRICTED DATA~~

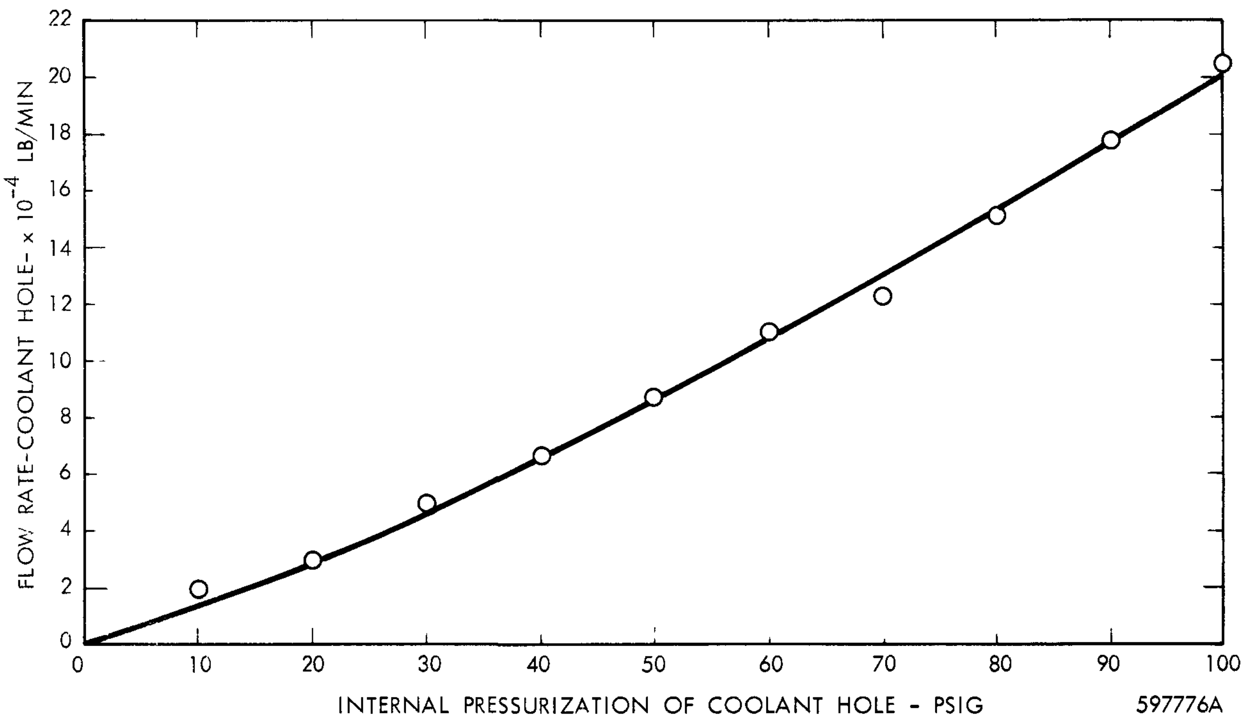

INNER REFLECTOR COOLANT HOLE POROUS FLOW TEST, INTERNAL PRESSURIZATION OF COOLANT HOLE, NITROGEN GAS ENVIRONMENT

Figure 19

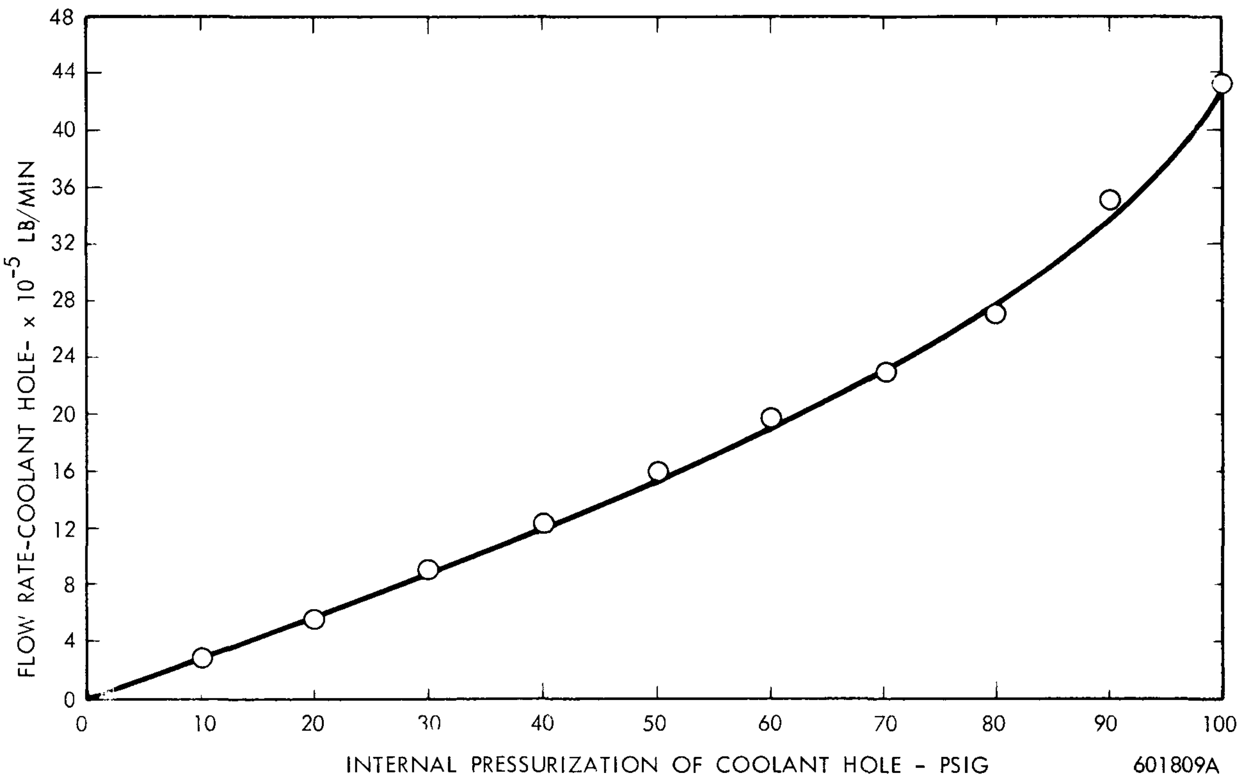

INNER REFLECTOR COOLANT HOLE POROUS FLOW TEST, INTERNAL PRESSURIZATION OF COOLANT HOLE, HYDROGEN GAS ENVIRONMENT

Figure 20

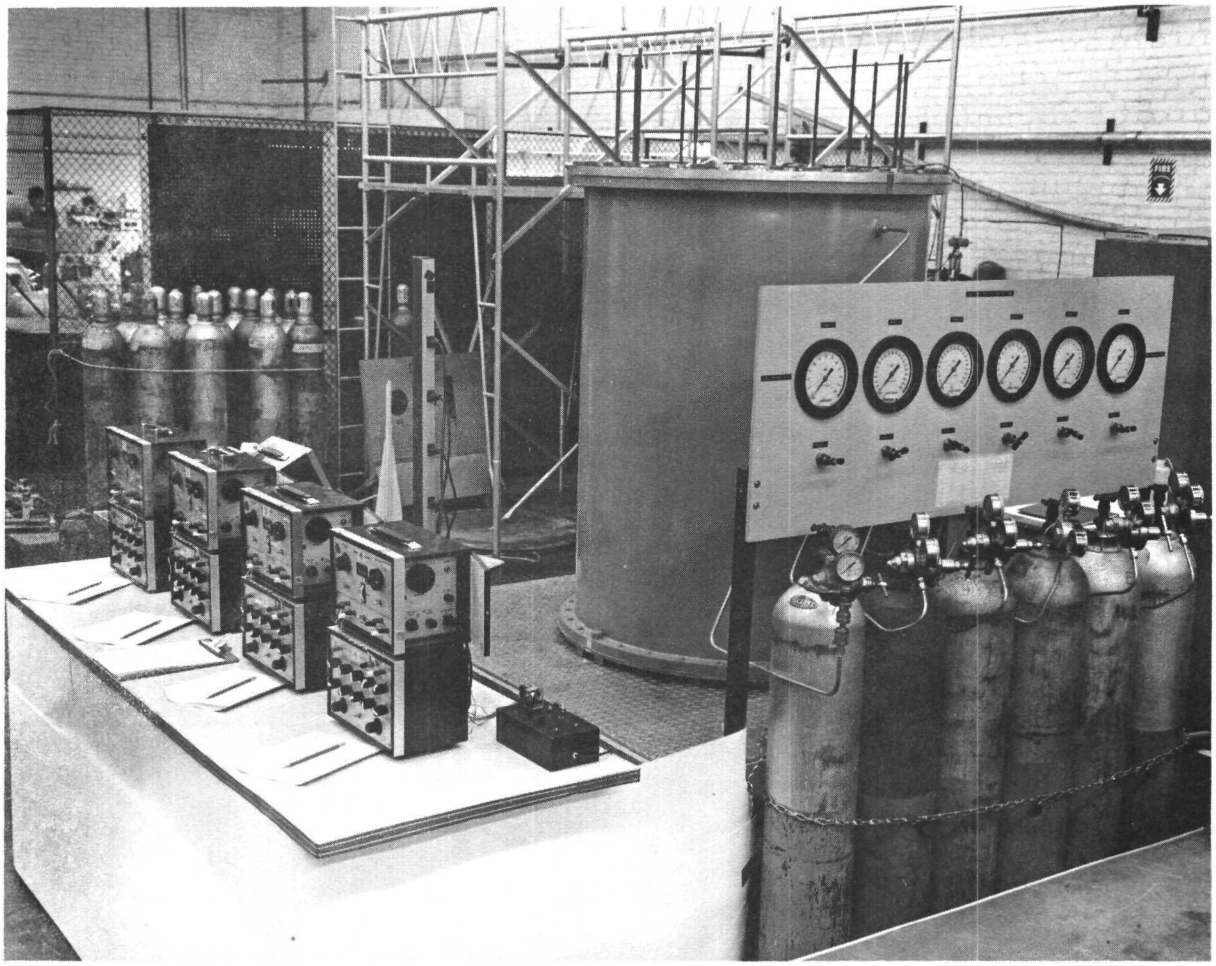

Figure 21
Test Setup for the Inner Reflector Graphite Cylinder
(Permeability and Buckling Tests)

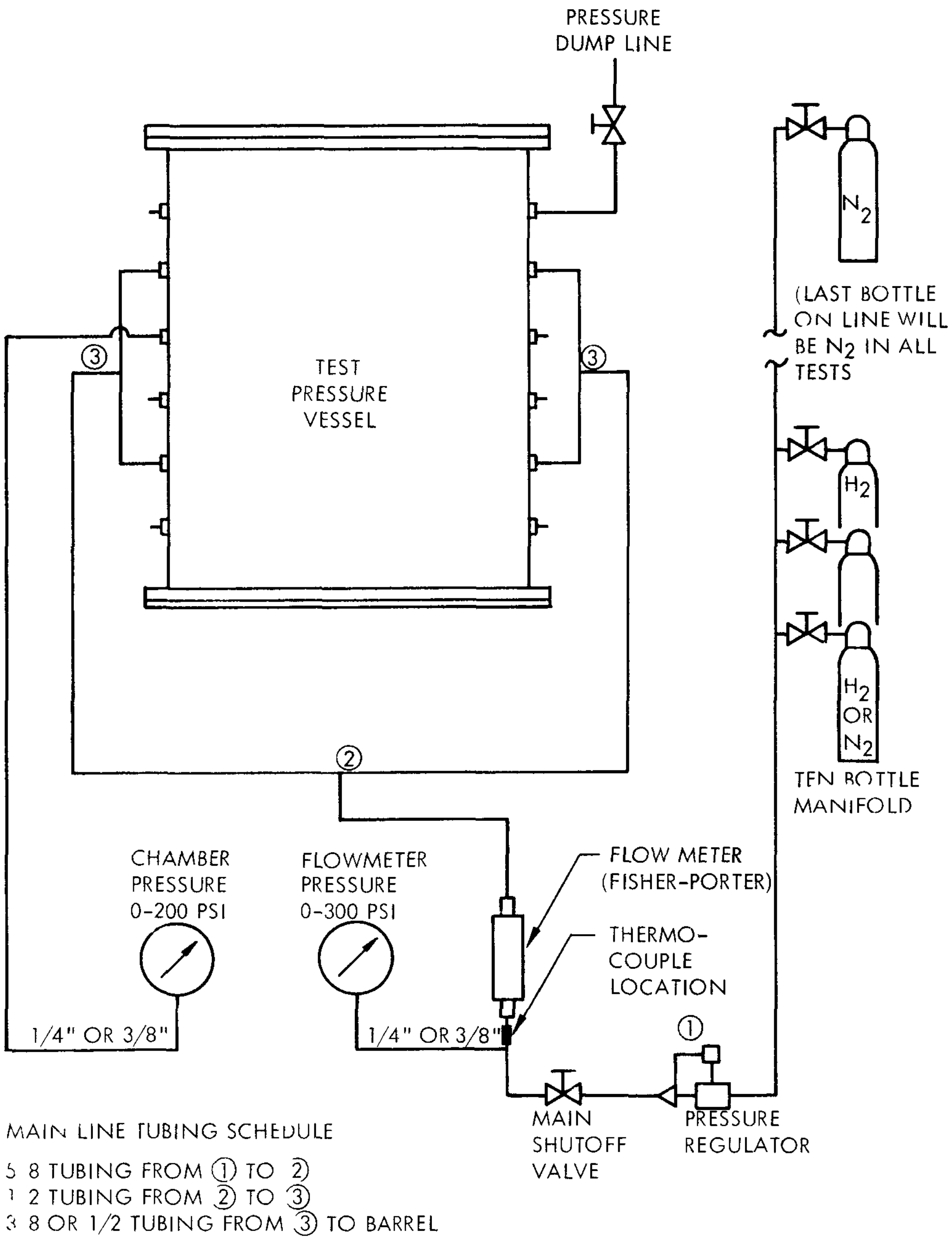

597764A

TEST PRESSURE VESSEL AND ASSOCIATED EQUIPMENT FOR PRESSURIZATION OF INNER REFLECTOR CYLINDER

Figure 22

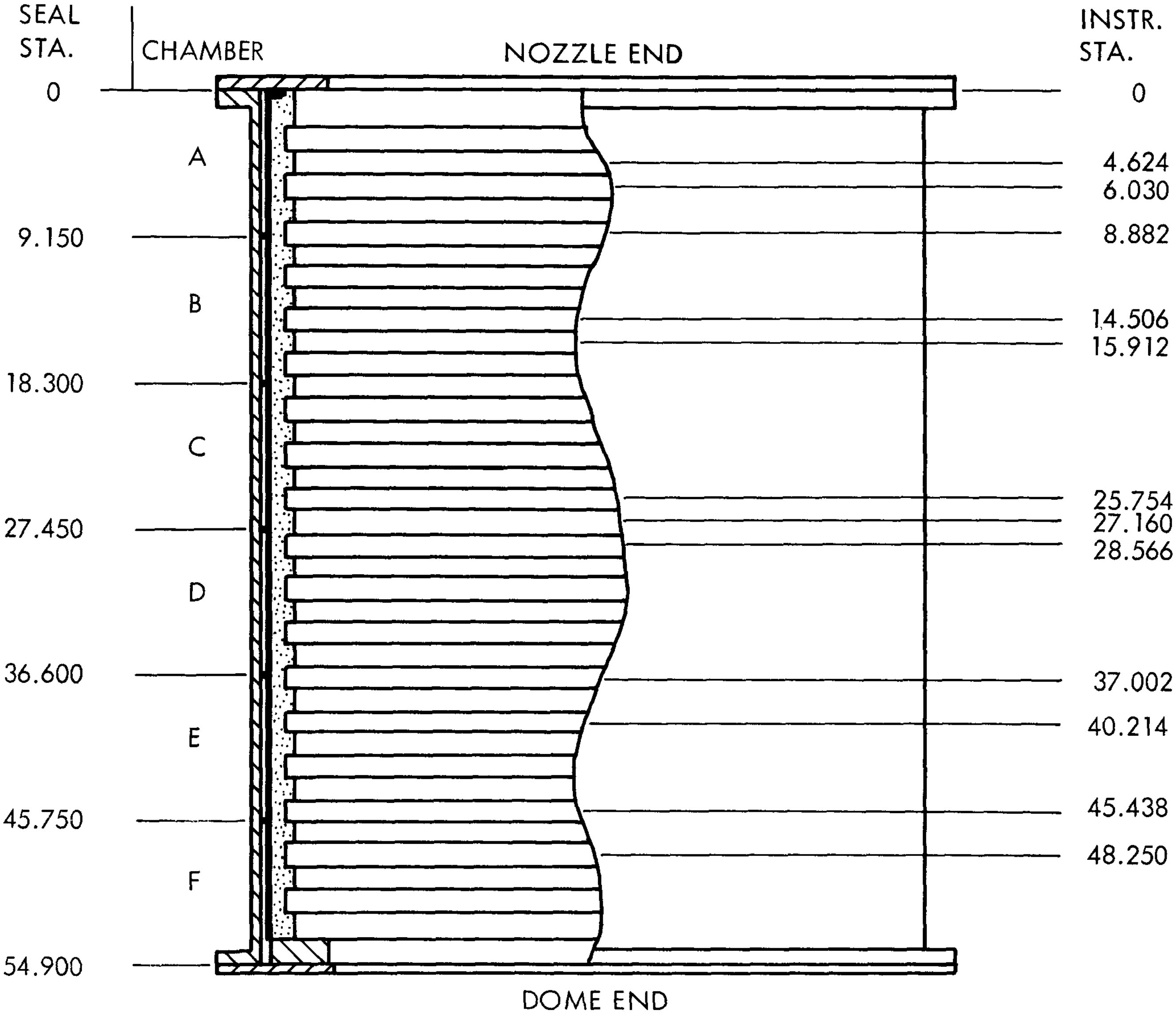

601817A

PRESSURE CHAMBER AND INSTRUMENTATION

LOCATION

Figure 23 Sheet 1

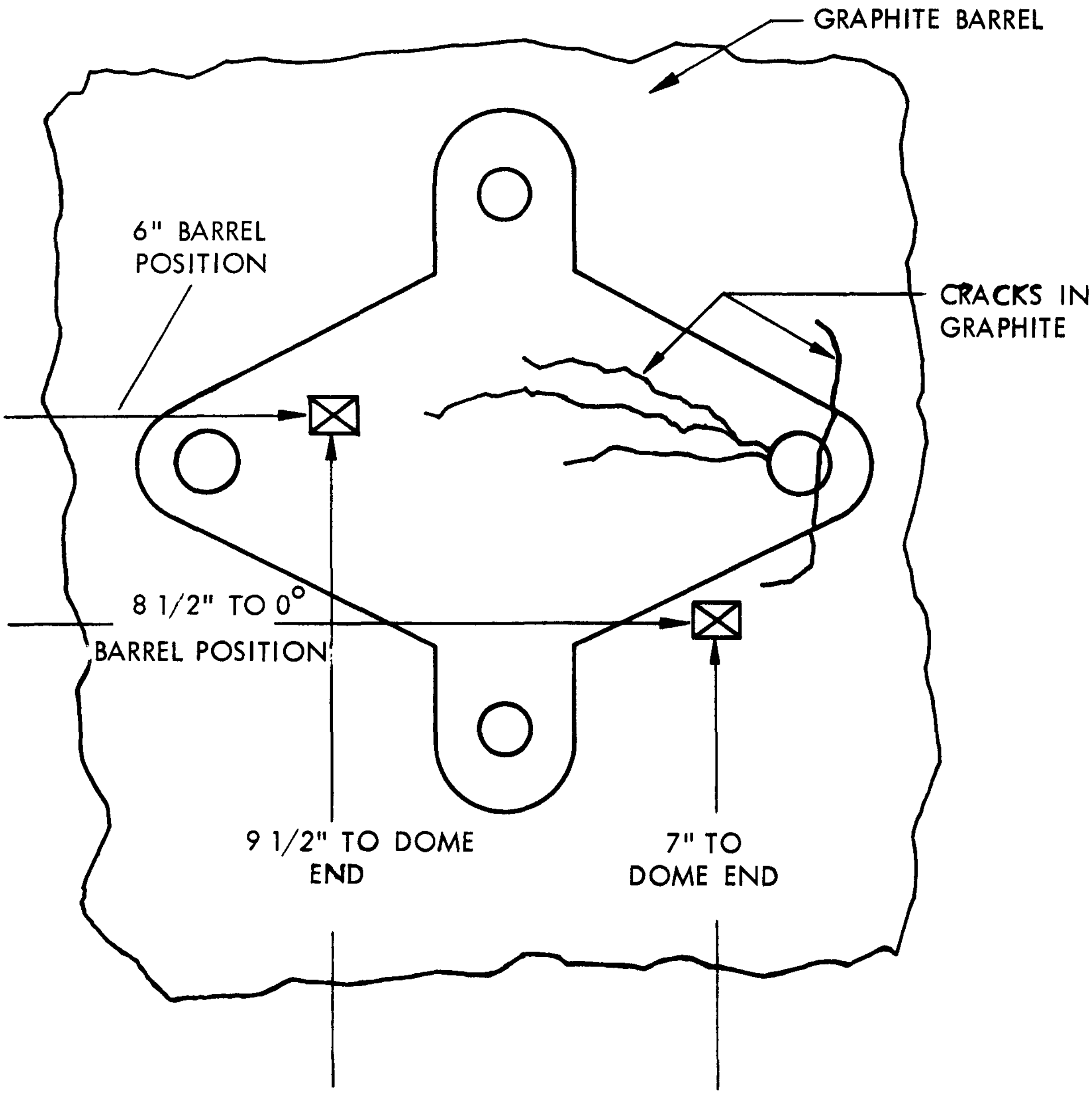

STRAIN GAGE LOCATION NEAR CRACKED AREA OF INNER REFLECTOR

597763A

Figure 23 Sheet 2

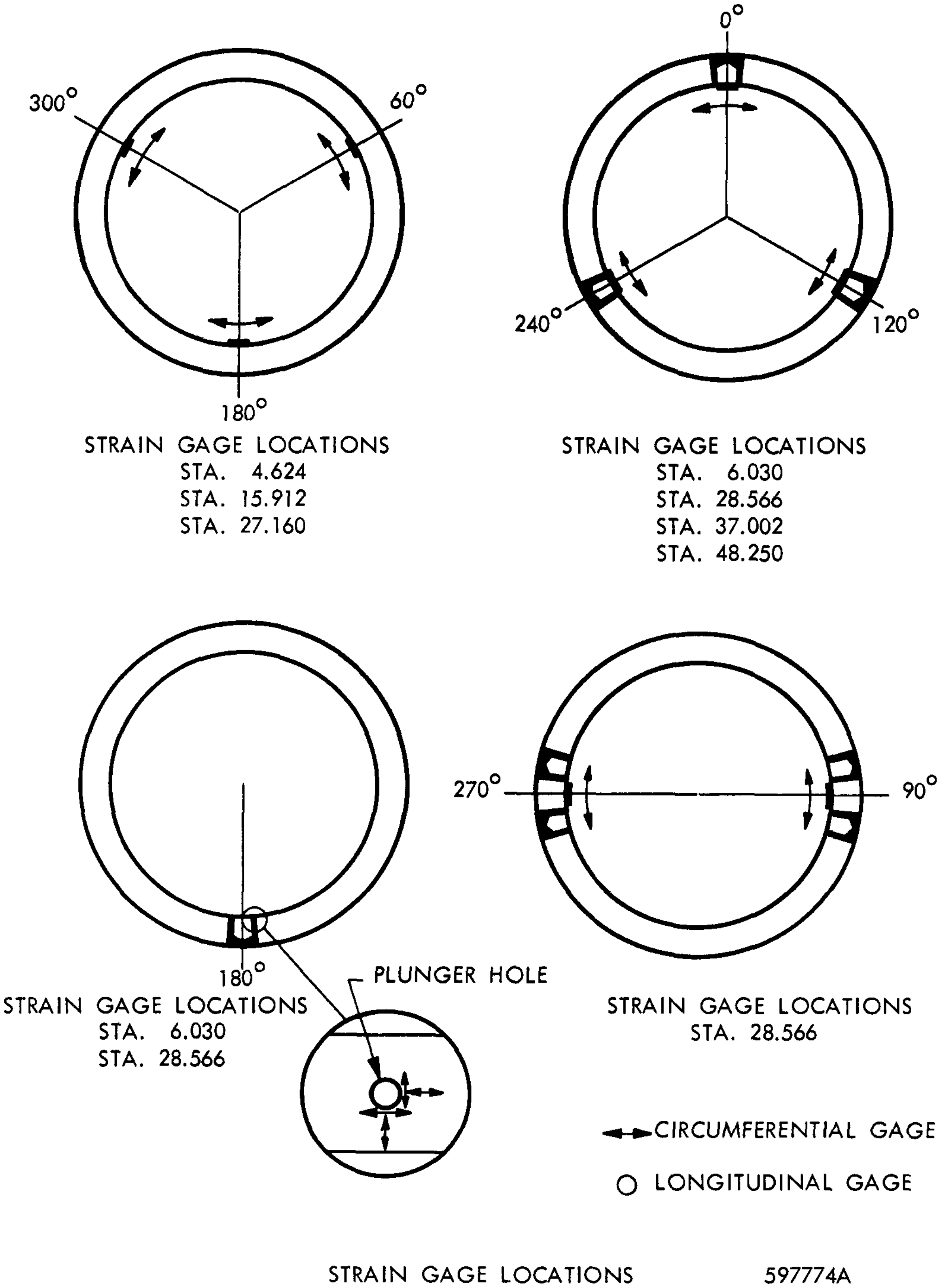

STRAIN GAGE LOCATIONS 597774A

Figure 23 Sheet 3

[redacted]

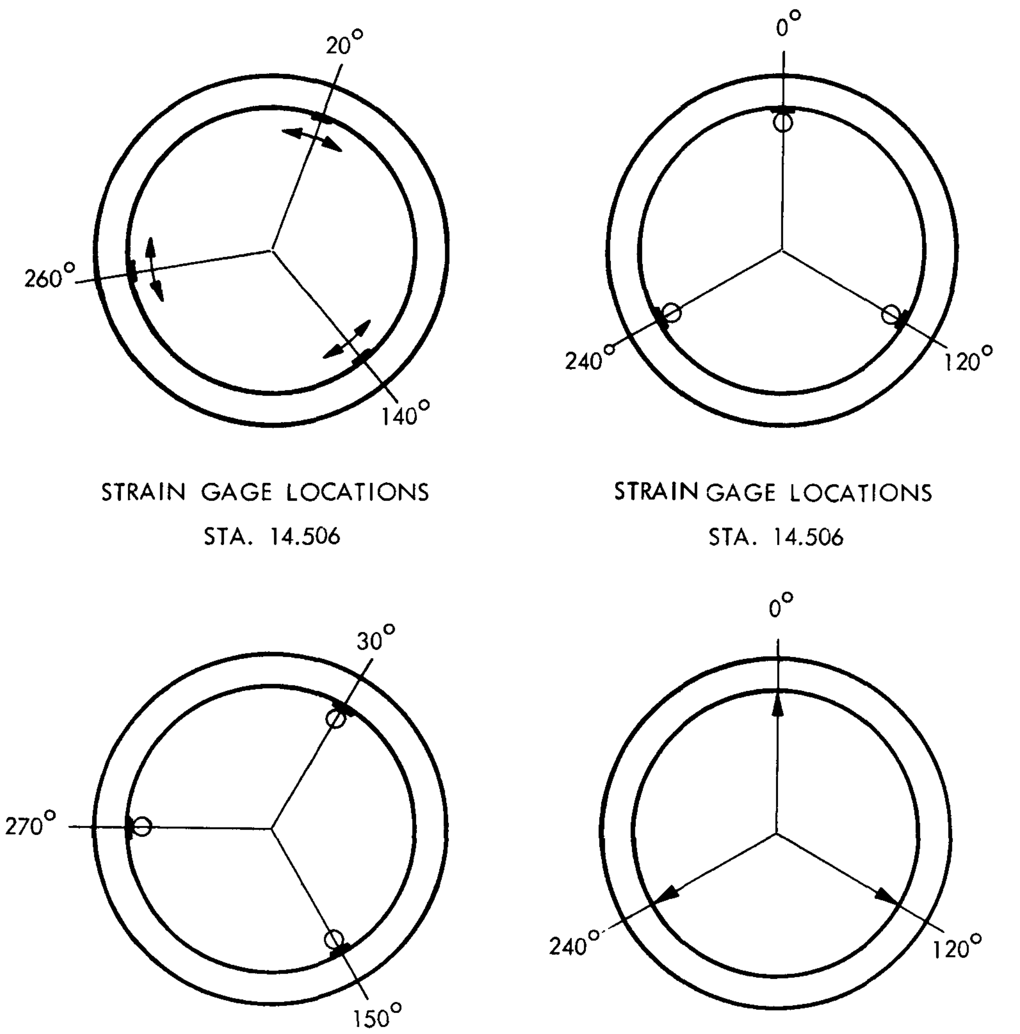

STRAIN GAGE LOCATIONS
STA. 14.506

STRAIN GAGE LOCATIONS
STA. 14.506

STRAIN GAGE LOCATIONS
STA. 37.002

LVDT LOCATIONS
STA. 8.882
STA. 25.754
STA. 45.438

↔ CIRCUMFERENTIAL GAGE
○ LONGITUDINAL GAGE

STRAIN GAGE AND LVDT LOCATIONS 597773A

Figure 23 Sheet 4

[redacted]

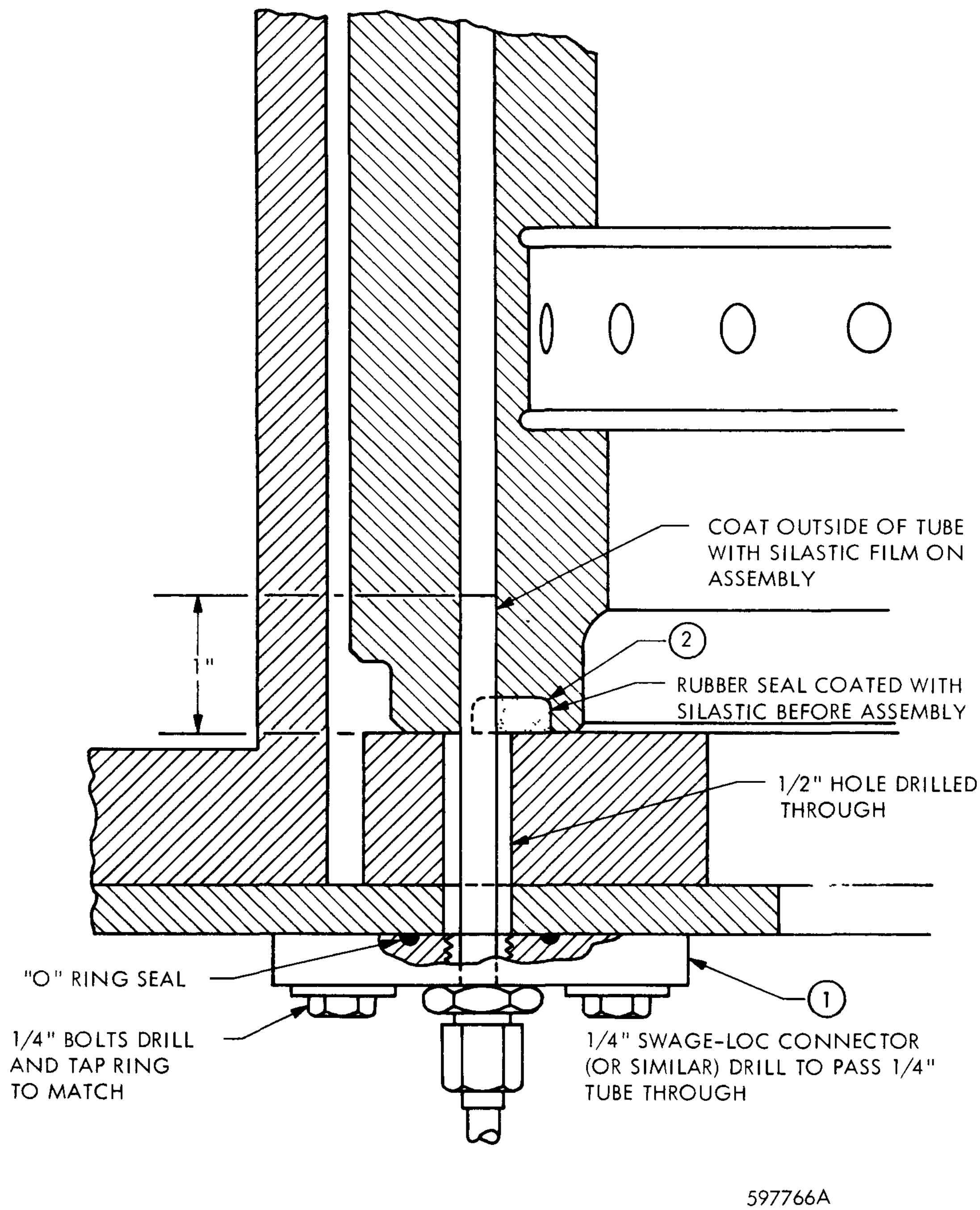

MODIFIED TEST ASSEMBLY FOR COOLING HOLE TEST

Figure 24

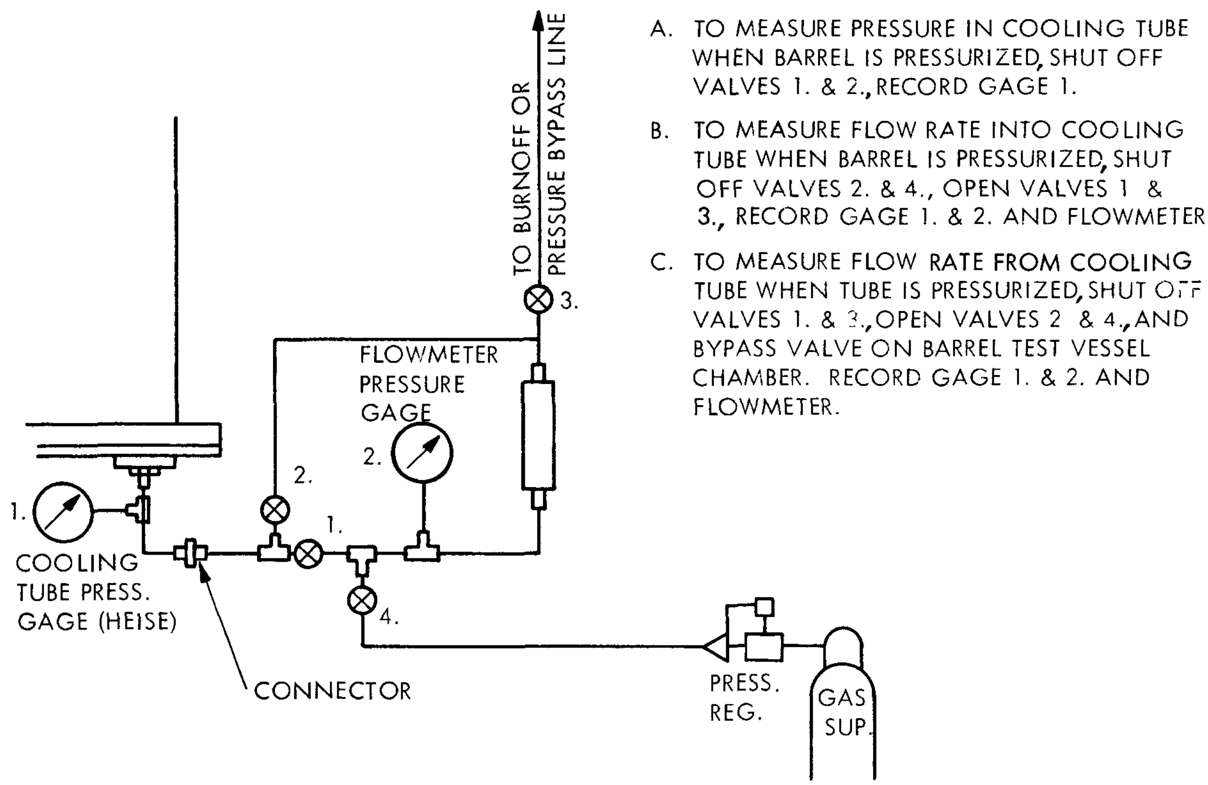

INSTRUMENTATION SET-UP FOR COOLING HOLE TEST

Figure 25

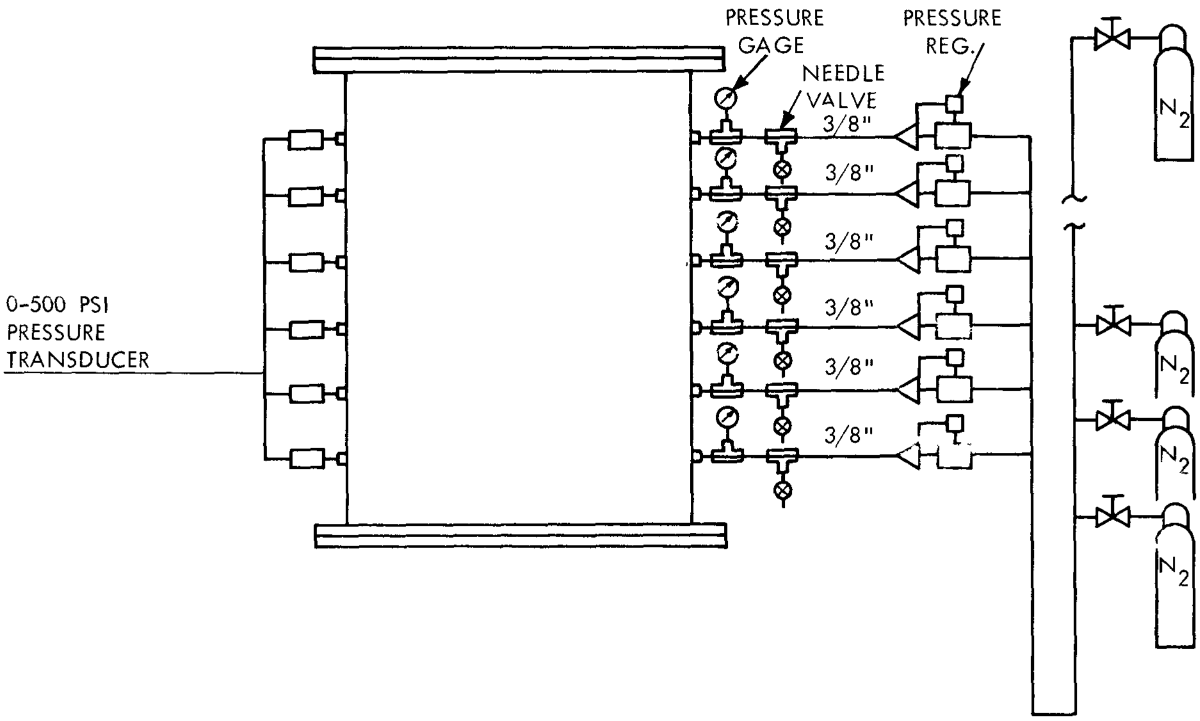

SCHEMATIC FOR APPLYING A RAMP PRESSURE PROFILE TO THE INNER REFLECTOR AND ENCOMPASSING ALUMINUM BARREL

597765A

Figure 26

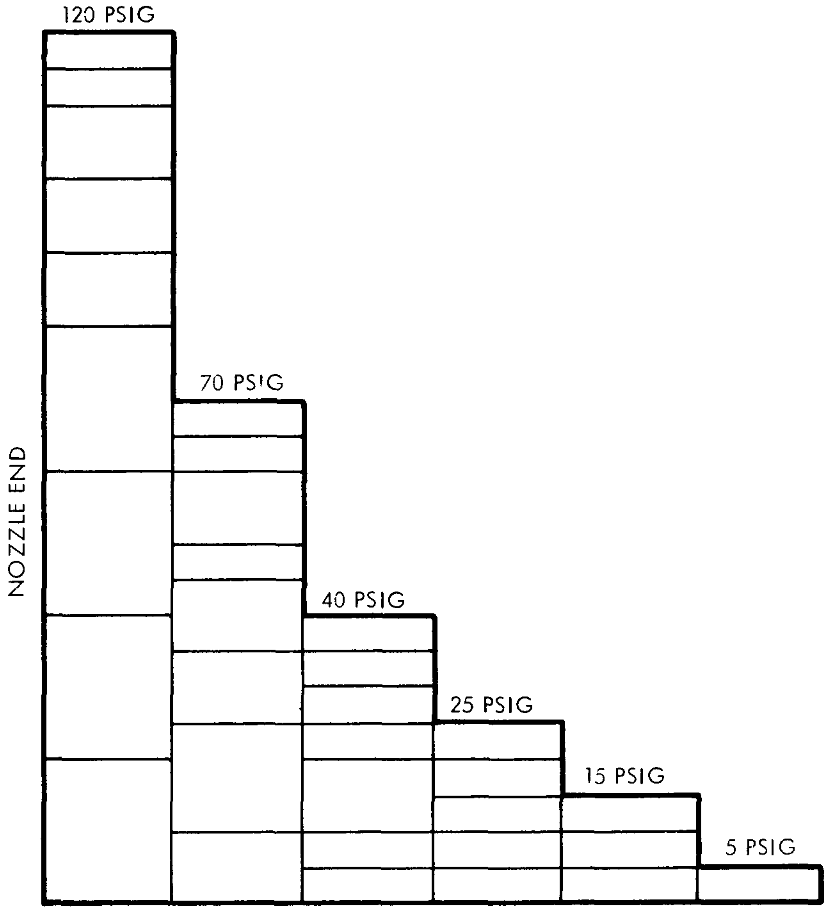

TEST STEP	TEST VESSEL COMPARTMENT					
	A	B	C	D	E	F
1	20	10	5	5	0	0
2	40	25	10	10	5	0
3	60	35	20	10	5	0
4	80	45	25	15	10	5
5	90	50	30	15	10	5
6	100	60	35	20	10	5
7	110	65	35	20	15	5
8	115	70	40	25	15	5
9	120	70	40	25	15	5

597769A

PRESSURE PROFILE TO SIMULATE NRX-A1 OPERATING CONDITIONS (BUCKLING TEST)

Figure 27 Sheet 1

~~CONFIDENTIAL~~
~~RESTRICTED DATA~~
[redacted]

Astronuclear

WANL-TME-768

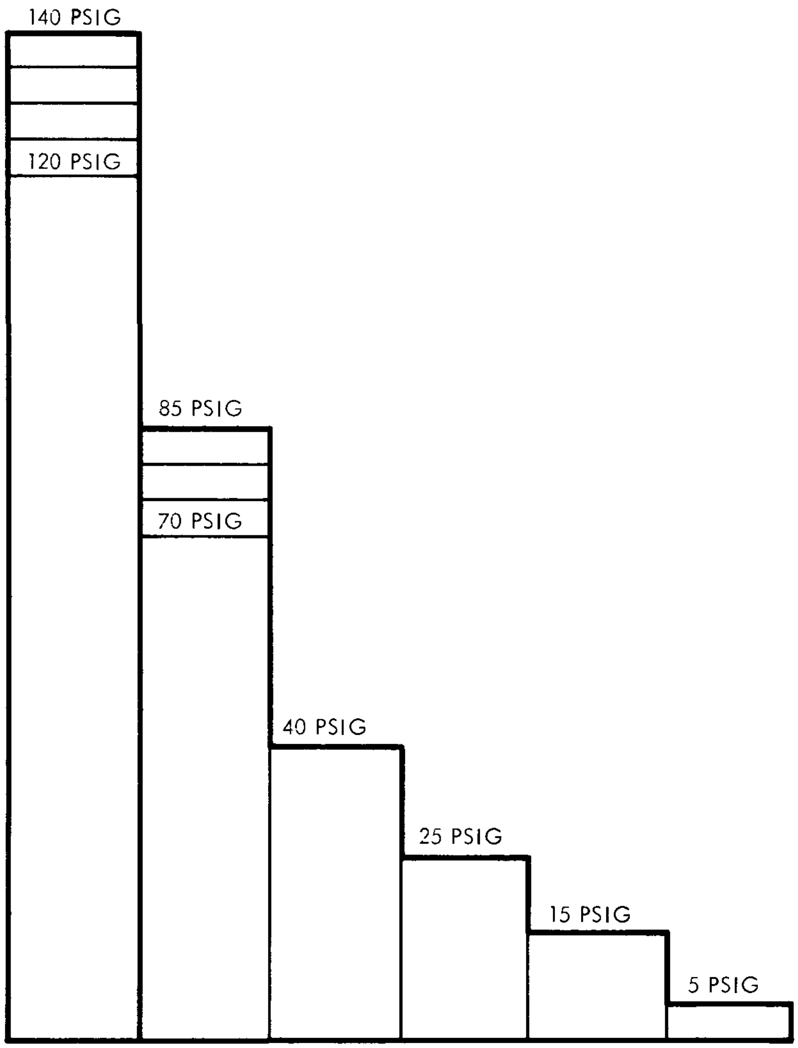

TEST STEP	TEST VESSEL COMPARTMENT					
	A	B	C	D	E	F
*9	120	70	40	25	15	5
10	125	75	40	25	15	5
11	130	80	40	25	15	5
12	135	80	40	25	15	5
13	140	85	40	25	15	5

*FROM PRESSURE PROFILE FOR 25 LB/SEC STRAIGHT FLOW, JANUARY 2, 1964

597770A

PRESSURE PROFILE FOR SPLIT FLOW; DOME FLOW 13 lb/sec, CORE FLOW 38 lb/sec

BUCKLING TEST

Figure 27 Sheet 2

~~CONFIDENTIAL~~
~~RESTRICTED DATA~~
[redacted]

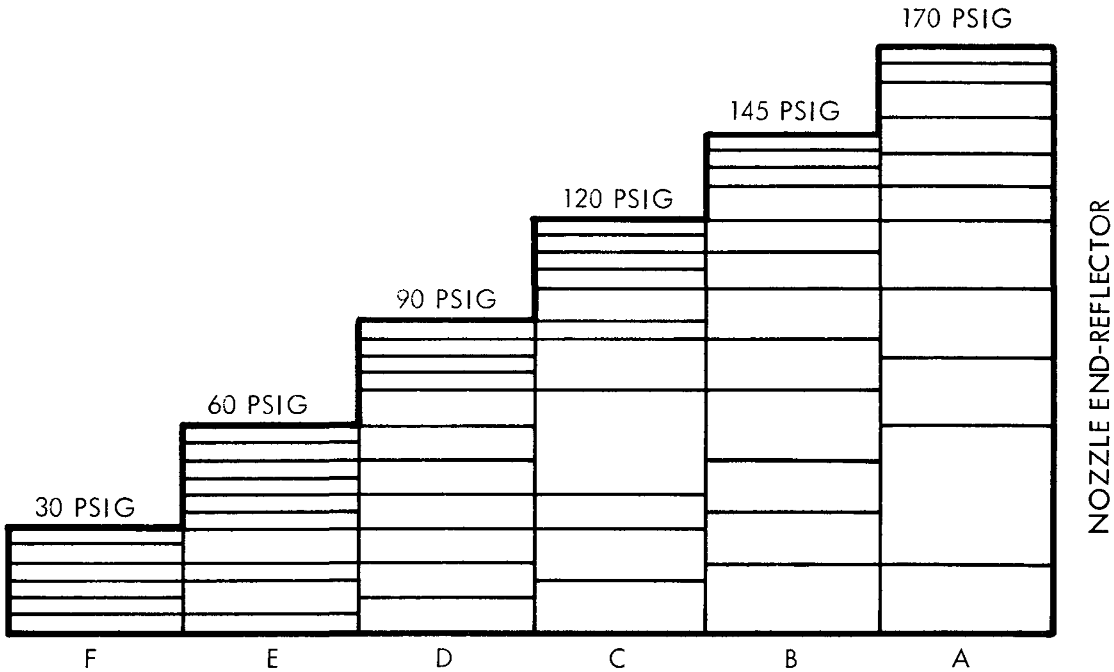

TEST STEP	TEST VESSEL COMPARTMENT					
	A	B	C	D	E	F
1	20	20	15	10	5	5
2	40	35	30	20	15	5
3	60	50	40	30	20	10
4	80	70	55	40	30	15
5	100	85	70	50	35	15
6	120	100	85	60	40	20
7	130	110	90	70	45	20
8	140	120	100	75	50	25
9	150	130	105	80	50	25
10	160	135	110	85	55	25
11	165	140	115	90	55	30
12	170	145	120	90	60	30

597771A

RAMP PRESSURE PROFILE SIMULATING REACTOR FULL POWER OPERATING CONDITIONS

Figure 28

TABLE I

PERMEABILITY TEST OF
INNER REFLECTOR GRAPHITE BARREL

PRESSURE (psig)	NITROGEN FLOW RATE (lb/min)	HYDROGEN FLOW RATE (lb/min)
0		
10	.029	.0075
20	.058	No Reading Taken
30	.088	.020
50	.155	.0385
60	No Reading Taken	.0405
70	No Reading Taken	.0615
80	.283	.070
90	No Reading Taken	.083
100	.376	.092
110	.428	
120	.481	
130	.545	
140	.594	

TABLE II
INNER REFLECTOR GRAPHITE CYLINDER STRAIN AND DEFLECTION DATA
PERMEABILITY AND BUCKLING TESTS

STRAIN GAGE LOCATION	EXTERNAL PRESSURE - psig																					
	0	10	20	30	40	50	60	70	80	90	100	110	120	130	140	150	160	170	180	190	200	Units
Sta. 6.030 - 0° Cir.	0	129	170	363	---	622	779	923	1017	1190	1307	1388	1559	1681	1842	2009	2124	2359	2611	2869	2979	μ in./in.
Sta. 6.030 - 120° Cir.	0	125	227	377	---	619	745	876	989	1140	1228	1341	1482	1615	1776	1935	2063	2260	2456	2613	2613	"
Sta. 6.030 - 240° Cir.	0	122	218	366	---	597	738	868	973	1132	1258	1288	1509	1597	1806	1966	2136	2337	2559	2740	3164	"
Sta. 4.624 - 60° Cir.	0	124	156	432	---	664	884	995	1094	1302	1450	1488	1678	1837	2026	2208	2300	2593	2906	3299	4121	"
Sta. 4.624 - 180° Cir.	0	112	123	359	---	591	744	861	962	1114	1207	1292	1506	1563	1706	1854	2037	2269	2512	2775	3214	"
Sta. 4.624 - 300° Cir.	0	126	195	411	---	687	849	976	1106	1276	1423	1509	1710	1804	1968	2122	2332	2556	2796	3027	3169	"
Sta. 28.566 - 0° Cir.	0	120	273	340	---	595	695	815	960	1077	1244	1404	1595	1749	1908	2082	2248	2463	2717	2952	3089	"
Sta. 28.566 - 120° Cir.	0	102	139	314	---	549	632	744	871	973	1127	1296	1324	1570	1715	1866	1993	2174	2373	2501	2557	"
Sta. 28.566 - 240° Cir.	0	113	237	312	---	579	771	853	965	1031	1232	1505	1694	1873	2078	2281	2442	2660	2938	3216	3573	"
Sta. 27.160 - 60° Cir.	0	129	142	443	---	749	968	1089	1238	1424	1507	1580	1857	1936	2082	2127	2362	2684	3031	3674	4066	"
Sta. 27.160 - 180° Cir.	0	123	220	344	---	527	783	896	1029	1196	1316	1391	1596	1725	1882	2057	2198	2412	2665	2918	3404	"
Sta. 27.160 - 300° Cir.	0	132	162	366	---	606	746	852	974	1126	1265	1396	1529	1649	1787	1930	2075	2269	2470	2561	2701	"
Sta. 48.250 - 0° Cir.	0	141	252	438	---	734	895	1058	1207	1401	1549	1644	1885	2028	2264	2535	2719	2976	3295	3593	3930	"
Sta. 48.250 - 120° Cir.	0	128	237	382	---	660	797	943	1095	1266	1377	1381	1686	1854	2096	2304	2410	2647	2903	3140	3298	"
Sta. 48.250 - 240° Cir.	0	142	237	430	---	880	913	1038	1171	1368	1506	1578	1838	1977	2221	2483	2620	2881	3365	3466	3899	"
Sta. 40.214 - 325° Cir.	0	166	257	428	---	713	865	1015	1192	1334	1498	1638	1828	2050	2259	2464	2554	2813	3072	3312	3312	"
Sta. 45.438 - 330° Cir.*	0	129	273	402	---	621	---	---	999	----	1277	1423	1635	1938	3134	3437	----	----	----	----	----	"
Sta. 45.438 - 330° Cir.**	0	---	---	---	---	782	---	---	1297	----	1560	1747	1934	2122	2330	2538	2850	3266	3640	3973	3952	"
Sta. 45.438 - 335° Cir.	0	128	243	369	---	652	761	902	1037	1172	1321	1450	1598	1786	1962	2140	2257	2438	2620	2801	2740	"
Sta. 8.882 - 0° Rad.**	0	---	.58	---	---	1.47	---	---	2.55	---	3.37	3.79	4.18	4.61	5.07	5.53	6.23	7.0	7.86	8.63	12.81	$\times 10^{-2}$ in.
Sta. 25.754 - 0° Rad.**	0	---	.48	---	---	1.22	---	---	2.13	---	2.80	3.16	3.52	3.87	4.27	4.70	5.37	6.24	6.83	6.99	7.74	$\times 10^{-2}$ in.
Sta. 25.754 - 120° Rad.**	0	---	.43	---	---	1.24	---	---	2.60	---	3.04	3.44	3.84	4.28	4.83	5.45	6.48	7.76	9.22	11.13	17.75	$\times 10^{-2}$ in.
Sta. 25.754 - 240° Rad.**	0	---	.29	---	---	0.67	---	---	.99	---	1.06	1.14	1.18	1.22	1.22	1.14	0.87	0.47	-.23	-1.38	----	$\times 10^{-2}$ in.
Sta. 45.438 - 0° Rad.**	0	---	.45	---	---	1.14	---	---	1.94	---	2.51	2.74	3.04	3.31	3.57	3.95	4.52	5.40	6.27	7.03	10.15	$\times 10^{-2}$ in.

Notes: (1) * Uniform pressurization of reflector. First buckling test run (0 to 150 psig). Cracked Area
(2) ** Uniform pressurization of reflector. Second buckling test run (0 to 200 psig). Cracked Area
(3) *Refer to Figure 23 for station location.*
(4) Unless specified otherwise, all strain data are average values obtained during permeability and buckling tests.
(5) Deflection readings above .100 in. are questionable due to the non-linearity of the instrumentation.

TABLE III

INNER REFLECTOR GRAPHITE CYLINDER
STRESS CONCENTRATIONS AROUND PLUNGER HOLES
BUCKLING TEST

UNIFORM EXTERNAL PRESSURE (psig)	CIRCUMFERENTIAL STRAIN (μ in./in.)					
	Station 6.030			Station 28.566		
	GROSS MAT'L.	PLUNGER HOLE		GROSS MAT'L.	PLUNGER HOLE	
	240°	180° SH	180° BH	240°	180° SH	180° BH
0	0	0	0	0	0	0
10	122	---	---	113	---	---
20	218	---	---	237	---	---
30	366	---	---	312	---	---
40	---	---	---	---	---	---
50	597	201	639	579	190	577
60	738	---	---	853	---	---
70	868	---	---	771	---	---
80	973	342	1116	965	332	1059
90	1132	---	----	1031	---	----
100	1258	435	1448	1232	428	1385
110	1285	483	1624	1505	481	1570
120	1509	531	1793	1694	530	1741
130	1597	581	1973	1873	577	1927
140	1806	633	2154	2078	628	2116
150	1966	682	2350	2281	685	2311
160	2136	749	2603	2442	750	2578
170	2337	819	2873	2660	820	2854
180	2559	888	3163	2938	890	3160
190	2704	959	3442	3216	955	3451
200	3164	1055	3795	3573	1064	3854

Notes:
(1) Refer to Figure 23 for station location.
(2) BH - Bottom of plunger hole.
(3) SH - Side of plunger hole.
(4) Circumferential strain with respect to the inner reflector cylinder.

TABLE IV

INNER REFLECTOR COOLANT HOLE POROUS FLOW TEST
NITROGEN GAS ENVIRONMENT

External Pressurization of Inner Reflector

External Pressure (psig)	Gross Flow Rate lb/min	Coolant Hole Pressure (psig)	Coolant Hole Flow Rate lb/min
0	0	0	0
10	.034	7.3	.00105
20	.071	17.2	.00319
30	.106	26.4	.00511
40	.140	35.5	.00701
50	.180	44.6	.00939
60	.227	54.1	.01310
70	.273	63.8	.0170
80	.326	73.2	.0211
90	.372	82.9	.0264
100	.427	92.0	.0320

Internal Pressurization of Coolant Hole

Coolant Hole Pressure (psig)	Coolant Hole Flow Rate lb/min
0	0
10	.00019
20	.00030
30	.00050
40	.00067
50	.00088
60	.00111
70	.00123
80	.00152
90	.00178
100	.00205

TABLE V

INNER REFLECTOR COOLANT HOLE POROUS FLOW TEST
HYDROGEN GAS ENVIRONMENT

External Pressurization of Inner Reflector

External Pressure (psig)	Gross Flow Rate lb/min	Coolant Hole Pressure (psig)	Coolant Hole Flow Rate lb/min
10	.0067	8.5	.000020
20	.0143	16.9	.000086
30	.0242	25.9	.00017
40	.0312	35.0	.00027
50	.0414	44.4	.00042
60	.0513	53.6	.00064
70	.0618	63.3	.00073
80	.0739	72.7	.00095
90	.0860	82.5	.00119
100	.0995	91.6	.00140

Internal Pressurization of Coolant Hole

Coolant Hole Pressure (psig)	Coolant Hole Flow Rate lb/min
0	0
10	.000030
20	.000056
30	.000090
40	.000123
50	.000160
60	.000199
70	.000232
80	.000272
90	.000353
100	.000435